UNIVERSITEIT VAN PRETORIA
UNIVERSITY OF PRETORIA
YUNIBESITHI YA PRETORIA

Low-field microwave absorption in pulsed lased deposited FeSi thin films

by

Happyson Michael Gavi

Submitted in partial fulfillment of the requirements for the degree of

MAGISTER SCIENTIAE

in the Faculty of Natural and Agriculture Sciences at the University of Pretoria

September……2011

Supervisor/Promoter: Dr. N. Manyala

Co-supervisor: Prof. V.V. Srinivasu

Summary

Low-field microwave absorption in pulsed lased deposited FeSi thin films

by

Happyson Michael Gavi

Submitted in partial fulfillment of the requirements for the degree of (MSc) in Physics in the Faculty of Natural and Agricultural Science, University of Pretoria

Supervisor/Promoter: Dr. N. Manyala

Co-Supervisor: Prof. V.V. Srinivasu

The magnetic behavior of cubic B20 crystal structure FeSi thin film has been previously probed at macroscopic level using a magnetometer. The results revealed ferromagnetic state with significant hysteresis. This is contrary to the bulk with the same cubic B20 crystal structure that is paramagnetic. The origin of ferromagnetism in thin films in contrast to paramagnetism in the bulk is unclear and unexplained.

Electron spin resonance technique (ESR) was used as a tool to characterize the magnetic behavior of FeSi thin films at microscopic level. With ESR technique, B20 crystalline FeSi show microwave power absorption centred at zero field (H_{DC} = 0) termed low-field microwave absorption (LFA) in addition to usual ferromagnetic resonance (FMR) typical of magnetic materials.

LFA was observed as a distinct signal in these films. This signal has been observed in several other materials other than FeSi thin films. However in FeSi thin films it was for the first time that LFA signal was observed. The LFA is closely connected to the magnetization process that occurs at low applied field. LFA is a new technique that has recently been used to detect the magnetic transition in materials, sensitive detection of magnetic order and more importantly to distinguish between different dynamics of microwave absorption centres.

The LFA measurements were made at 9.4 GHz (X-band) on pulse laser deposited (PLD) polycrystalline B20 cubic structure FeSi thin film grown on Si (111) substrate. PLD is regarded as a powerful tool for thin film growth. The LFA properties of the films were investigated as a function of DC field, temperature, microwave power and orientation of DC field with respect to the film surface. The LFA signal is very strong when the DC field is parallel to the film surface and diminishes at higher angles. This is attributed to induced anisotropy field (IAF) and surface anisotropy field (SAF) contributing to total anisotropy field (TAF). The LFA signal strength increases as the microwave power is increased, such increase is due to impedance and thus showing that LFA and magnetoimpedance (MI) has common origin. The LFA signal disappears around 340 K which can be attributed to the disappearance of long range order giving us a positive signature of surviving magnetic state well above room temperature in these films. We believe that domain structure evolution in low-fields, which in turn modifies the low field permeability as well as the anisotropy, could be the origin of LFA observed in these films. MI and LFA can be understood as the absorption of electromagnetic radiation by spin systems that are modified by domain configuration and strongly depend on anisotropy field. The observation of LFA opens the possibility of FeSi films to be used as potential candidates of low magnetic field sensors in the microwave and radio frequency regions.

UNIVERSITEIT VAN PRETORIA
UNIVERSITY OF PRETORIA
YUNIBESITHI YA PRETORIA

DECLARATION

I, Happyson Michael Gavi, declare that the thesis, which I hereby submit for the degree of MSc in Physics at the University of Pretoria is my own work and has not previously been submitted by me for a degree at this or any other tertiary institution.

Signature: ……

Date: …….

Acknowledgements

I would like to extend my sincere gratitude to the following people for their valuable contribution towards the completion of my MSc work.

- My academic supervisor, Dr. N. Manyala for his immortal guidance, discussions and support throughout this study.
- The Head of the Physics department, Prof. J. B. Malherbe for the part time teaching jobs which he organised for me to supplement my finances.
- My co-supervisor Prof. V.V. Srinivasu for the fruitful discussions, encouragement and suggestions in the compilation of this thesis.
- Dr Balla Ngom for his contributions in the synthesis of FeSi thin films.
- Financial assistance of the project provided by University of Pretoria research development program.
- Fellow senior students in the physics department, for their encouragement and moral support.
- My parents, my wife and my daughter for their eternal love and encouragement throughout my studies and beyond.

Table of contents

ABBREVIATIONS

AFM-Atomic Force Microscopy

AC-Alternating Current

CVD-Chemical Vapor Deposition

DC-Direct Current

ESR-Electron Spin Resonance

FMR-Ferromagnetic Resonance

GMI-Giant Magnetoimpedance

H_{DC}-DC static magnetic field

H_{AC}-AC microwave field

IAF-Induced Anisotropy Field

LFA-Low Field Microwave Absorption

MI-Magnetoimpedance

NWs-Nanowires

PLD-Pulse Laser Deposition

RBS-Rutherford Backscattering Spectroscopy

SAF-Surface Anisotropy Field

TAF-Total Anisotropy Field

(VLS) NW-Vapor Liquid Solid Nanowire growth

XRD-X-ray Diffraction

CHAPTER 1.

Introduction

In the last 60 years, considerable attention has been given to transition metal mono-silicides because they were found to possess a number of anomalous magnetic and electrical conducting properties [1]. Silicides have found application in microelectronics because of their large silicon content, high electrical conductivity, and high temperature stability and corrosion resistance. Transition metal mono-silicides can be prepared easily and reliably and reveal a potential for electronic application in-spite of ever-decreasing circuit dimensions in silicon (Si) integrated circuits. Moreover they provide a possibility of fabrication 3D circuit structures and faster heterostructure devices [2].

Among silicides, FeSi has recently gained particular significance since it behaves anomalously in various ways and hence can find diverse technological applications. The cubic B20 compound, FeSi is a non-magnetic narrow gap semiconductor at low temperatures. Its paramagnetic susceptibility $\chi(T)$ is small at low temperatures (≈ 100 K), but increases rapidly until it reaches a maximum at 500 K. Beyond 500 K it portrays Curie-Weiss behavior. An explanation for such behavior was proposed by Jacarino *et al* [3]. At high temperature (above 300 K) behaves like a dirty metal. Transition from semiconducting to metallic behavior is attributed probably from the narrow band gap in the material [4].

Numerous neutron diffraction techniques have been conducted to examine magnetic scattering in FeSi bulk samples. Powder diffraction showed that there was no antiferromagnetic ordering at liquid nitrogen temperatures [5]. Polarized neutron diffraction experiments with powders at 293 K and 850 K failed to identify any magnetic scattering but single-crystal polarized neutron work reveal very weak diffuse magnetic scattering arising from the temperature induced paramagnetism [6]. Magnetic susceptibility χ measurements conducted reveal that χ of single crystalline and polycrystalline FeSi approaches zero at temperature T < 100 K portraying non-magnetic state of the sample. Contrary to the bulk, FeSi films display χ measurements similar to disordered ferromagnets with significant history dependence [7]. This behavior is similar to soft

ferromagnets with a coercive field of ($\approx$100 Oe) and saturated magnetization M at higher fields H ($\approx$2000 Oe). Thin films of FeSi are promising candidates for spintronics applications where magnetic semiconducting films serve as injectors and collectors of spin polarized currents in Si transistors. Thin films portray a high Curie temperature T_C ($\approx$ 30 K) in contrast to the bulk with T_C ($\approx$ 0 K). The T_C of both the films and bulk samples was determined from the peak of zero magnetic field (H) cooled (ZFC) susceptibility measurements as a function of temperature [7].

Synthesis of single phase low dimensional (1-D) FeSi is challenging partially due to the complex phase diagram of Fe and Si which includes five known bulk phases (Fe_2Si, Fe_5Si_3, FeSi, $\alpha-FeSi_2$ and $\beta-FeSi_2$) [8]. However, growth of free standing FeSi nanowires (NWs) by chemical vapor deposition methods (CVD) has been reported [9]. Unlike vapor-liquid-solid (VLS) NW growth, FeSi nanowires (NWs) form without the inclusion of metal catalysts and strongly depend on the surface employed [10]. One dimensional inorganic (1-D) NW materials have gained prominent attention in the past decade since they have found many promising applications, such as in electronics, photonics, spintronics, sensing, photovoltaics and thermoelectrics [11, 12].

The films used on this study were grown on Si (111) substrate with cubic B20 structure using pulse laser deposition method (PLD) with structural properties similar to the bulk [7]. The use of PLD offers numerous advantages over the use of other deposition techniques. PLD does not require multiple step deposition procedures as in the template technique nor does it require large thermal budget in order to affect mass transport over long distances as does solid phase epitaxy (SPE). Moreover, PLD offers precise stoichiometry transfer from the target to the substrate. Previous studies have shown that the stoichiometry of PLD films is similar to that of the ablation target [13, 14]. However the quality of the FeSi films may have been affected by the higher kinetic energies of the ablated flux as well as by different chemical species which could be produced during the ablation process. Structure and morphology of the films was effectively characterized [7]. X-ray diffraction, transmission electron and atomic force microscopies reveal films to be dense, very smooth, and single-crystalline cubic B20 FeSi. X-ray diffraction (XRD) measurements reveal a lattice constant *a* that is 0.3 % larger in thin films than for the bulk FeSi. Such differences might be the key to the significant difference in magnetic properties between the two parties. Another cause may be attributed to small variations in the Fe to Si ratio although Rutherford backscattering spectroscopy (RBS) and x-ray fluorescence (EDX) confirm

stoichiometry of the films to be within 50-50% or 1:1 within experimental error of about 2%. However it should be noted that stoichiometry is averaged over large film areas and local variations are possible. The presence of Fe that has diffused into the substrate is not expected to contribute to magnetization M since Fe ions that are well co-ordinated with Si have approximately zero magnetic moments. Magnetic moment on Fe drops to zero when the Si content increases to 40 % and in this case Si content was 50 % [15]. The origin of ferromagnetism in thin films in contrast to paramagnetism in the bulk is unclear and unexplained. This led to the interest to probe magnetic properties of films at a microscopic level using electron spin resonance spectrometer (ESR). Previous work reported in reference 7 has probed magnetic properties of FeSi at a macroscopic level using magnetometer.

Our major objective with the ESR technique was to probe ferromagnetic resonance (FMR) in thin films. FMR is the absorption of microwave magnetic field by a ferromagnetic material, measured as a function of an applied DC magnetic field. FMR is a useful tool to characterize material parameters such as magnetization, magnetic anisotropy, high frequency loss, frozen in strain and magnetic inhomogeneity. However instead of observing high field microwave absorption associated with FMR, low field microwave absorption centered at zero magnetic field was observed. That absorption is understood to be connected to the magnetization process that occurs at low applied field although it has also some similar characteristics to the conventional FMR absorption [16]. The low-field microwave absorption properties of the FeSi thin films were then investigated as function of temperature, angle, and DC modulation field and microwave power. Low-field microwave absorption phenomenon was found to be dependent on the above mentioned parameters. The low-field microwave absorption measurement is very important since it is a novel phenomenon with various technological applications unfamiliar with many materials.

Microwave absorption centered at low field magnetic field B = 0 has been observed in several materials such as superconductors, silicate glasses, amorphous ferromagnetic ribbons and ferromagnetic oxides [17]. In all these cases a conclusion was drawn that the central influence of the low field microwave absorption (LFA) shape was the anisotropy field which makes LFA physically similar to giant magnetoimpedance (GMI). Furthermore, in some cases hysteresis was observed at magnetic field centered at B = 0 signifying the ferromagnetic state of a material.

We could not observe hysteresis in our research due to the limitations of our Jeol ESR spectrometer which could not capture the reverse sweep, though we actually see hysteresis along with the reverse sweep data on the instrument computer screen. Hysteresis can only be achieved if the DC static field is cycled in both the forward and reverse direction. LFA is non-resonant and non- Larmor phenomenon physically similar to GMI. A lot of work has been done to show a strong correlation between LFA and GMI [16]. Magnetoimpedance (MI) phenomenon has various technological applications very useful to modern-day society. However no research has been reported so far on low-field microwave absorption in FeSi thin films.

This study presents the results obtained from the electron spin resonance (ESR) spectrometer about microwave absorption properties of the thin films of FeSi prepared by pulse laser deposited (PLD) method. Low-field microwave absorption properties (LFA) of the thin films were investigated as a function of temperature, microwave power, DC modulation field and angle. An overview of the properties of FeSi as a Kondo insulator material is given in chapter 2 with particular reference to its crystal structure and magnetic properties. Information is given on magnetic properties of both thin films and the bulk FeSi.

Chapter 3 provides the theory of electron spin resonance (ESR) both in the higher and lower DC static magnetic field and the effect of temperature on ESR. This section explains that at higher DC static magnetic fields electron spin resonance will occur and at low DC static magnetic fields especially centered about B = 0 no resonance will occur. It is shown that higher DC static magnetic fields are usually associated with ferromagnetic resonance (FMR) if a material involved is ferromagnetic. Low DC static magnetic fields are associated with low-field microwave absorption (LFA). A strong theoretical correlation between low-field microwave absorption (LFA) and giant magnetoimpedance (GMI) is given in this section.

Chapter 4 gives details of the experimental set up and techniques that were employed in order to achieve the objectives of this study.

Chapter 5 summarises all the results obtained and discussed in this study.

References

[1] Y.Onose, N.Takeshita, C.Terakura, H.Takagi, and Y.Tokura, Phys. Rev**. B72,** 224431 (2005).

[2] S. Murarka, Intermetallics **3**, 173-186 (1995).

[3] V.Jaccarino, G.Wertheim, J.Wernick, L.Walker, and S.Arajs, Phys. Rev.160, 3 (1967).

[4] S.Evangelou and D.Edwards, J. Phys. C **16,** 2121 (1983).

[5] H. Watanabe, H. Yamamoto, and K. Ito , J. Phys. Soc. Jpn, **18**, 995-999 (1963).

[6] K. Motoya, M. Nishi, and Y. Ito, J. Phys. Soc. Jpn, **49**, 1631-1632 (1980).

[7] N. Manyala, B. Ngom, A. Beye, R. Bucher, M. Maaza, A. Strydom, A. Forbes, A. Johnson, and J. Ditusa, Appl. Phys. Lett. 94, 232503 (2009).

[8] L. Ouyang, E. Thrall, M. Deshmuck, and H. Park, Adv. Mater. (Weinheim, Ger.) **18**, 1437 (2006).

[9] H. Okamoto, Desk Handbook: Phase Diagrams for Binary Alloys; ASM International: Materials Park, OH, 2000.

[10] R. Wagner and W. Ellis. Appl. Phys. Lett, 4, 89-90 (1964).

[11] A. Schmitt, J. Higgins, J. Szczech, and S. Jin, J. Mater. Chem, 10, 1039 (2010).

[12] M. Bierman, and S. Jin, Energy & Environmental Science, 2, 1050-1059 (2009).

[13] P. Tiwari, M. Bahtnagar, R. Dat, and J. Narayan, Mater. Sci. Eng. B 14, 23 (1992).

[14] J. Cheung, and H. Sankur, CRC Critical Rev. Solid State Mater. Sci 15, 63 (1988).

[15] L. Haggstrom, A. Narayanasamy, T. Sundqvist, and A. Yosif, Solid State Commun., **44**, 1265-1267 (1982).

[16] M. Vazquez, G. Badidni-Confalonieri, and J. Torrejon; "Low-field microwave phenomena in CoFeSiB amorphous magnetic microwires"; IEE Third International Conference on Quantum, Nano and Micro Technologies (2009).

[15] R.Valenzuela, R. Zamorano, G. Alvarez, M. Gutierrez, and H. Montiel, J. Non-Cryst.Solids **353,** 768-772 (2007).

[17] D. de Cos, G. Alvarez, A. Garcia-Arribas, H. Montiel, J. Barandiaran, R. Zamorano, R. Valenzuela, Sens Acta A 142, 484-490 (2008).

CHAPTER 2: Survey of FeSi properties

2.1: Introduction

Transition metal monosilicides with B20 structure, MSi (M= Cr, Fe, Co, $Fe_{1-x}Co_x$) show a variety of interesting magnetic and transport properties and hence are promising candidates for technological applications. These materials have rich phase diagrams reflecting the great sensitivity with respect to changes in external control parameters like temperature, pressure and magnetic field. FeSi compound with B20 crystal structure has long attracted lots of interest because of the unusual temperature dependence of its various physical properties. Interest in iron monosilicides dates back to the late 30's when Foex had discovered that the magnetic susceptibility of this compound increased with temperature above 200K [1]. FeSi can be classified as a metal or semimetal since its resistivity (10^4 Ω cm) indicates a larger carrier concentration which is comparable in magnitude to other transition atom intermetallic compounds (e.g. V_3Si) [2]. Besides anomalous magnetism displayed by FeSi, this compound possesses superior electronic parameters such as high temperature stability, resistance to degradation and high electrical conductivity.

2.2: Crystal structure

Crystal structure of FeSi defines the structure formed when a basis of atoms (Fe and Si) is attached identically by every lattice point. A crystal structure formed when a basis of atoms (Fe and Si) is attached identically by every lattice point is a cubic B20 which can be viewed as distorted NaCl (B1) structure [3]. Individual atoms of Fe and Si are displaced from their positions in the B1 structure along the [111] directions so as to change NaCl third neighbor (i.e. along the cube diagonals) into FeSi nearest neighbors. The displacements reduce the space-group symmetry from F_m3_m (0_h^5) to $P2_13$ (T^4) in such a way that the Bravais lattice is a simple cubic but the overall point symmetry is tetrahedral [4]. Space group symmetry $P2_13$ (T^4) is illustrated in figure 1.1.

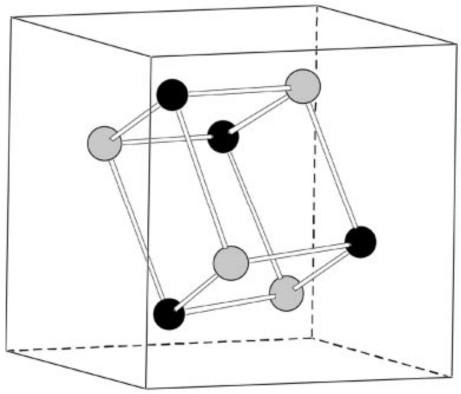

$P2_13$ (T^4)

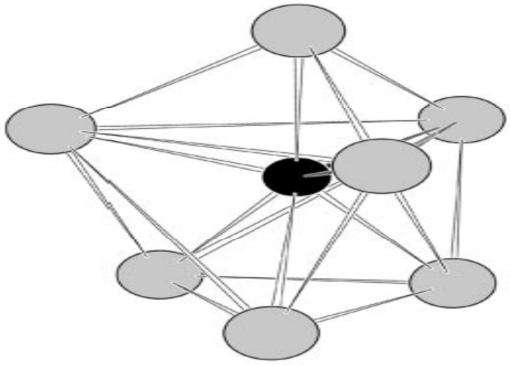

$TMSi_7$

Fig. 1.1: Crystal structure with the $P2_13$ (T^4) space group and a $TMSi_7$ cluster representing the site symmetry of individual atoms in this structure [5].

The $P2_13$ (T^4) space group has been reported in other compounds besides FeSi; such observations have been made in other 3d series compounds (CrSi, MnSi, CoSi, and NiSi). Moreover this space group has also been reported for RuSi, RhSi, ReSi and OsSi [5].

The B20 structure is fairly close packed with a 'touching sphere' volume ratio of 62% compared to 64% bcc [6]. FeSi has a cubic B20 structure at ambient conditions, where both the Fe and Si atoms are situated at the 4(a)-type sites in the simple cubic unit cell, with position co-ordinates (u_i, u_i, u_i), $(\frac{1}{2}+u_i, \frac{1}{2}-u_i, \bar{u}_i)$, $(\bar{u}_i, \frac{1}{2}+u_i, \frac{1}{2}-u_i)$ and $(\frac{1}{2}-u_i, \bar{u}_i, \frac{1}{2}+u_i)$ [7]. The cubic compound FeSi has eight atoms per unit cell. Each iron atom is surrounded by seven silicon atoms at the distances of 2.29 Å (one ligand in the [111] direction), 2.36 Å (3) and 2.53 Å (3) as illustrated in figure 1.2 [2]. The particularity of this structure is the seven-fold co-ordination for both the Fe and Si atoms; the seven-fold co-ordination is resembled by other transition-metal monosilicides that crystallize in the B20 phase (CrSi, MnSi, CoSi, and NiSi). However these transition-metal monosilicides have different electrical properties: CrSi and MnSi are metals; CoSi is a semimetal, while FeSi is a narrow-gap semiconductor [8].

The point symmetry at the Fe and Si sites is C_3 which is a cubic group of order 3 that consists of 120° rotations about an appropriate [111] axis and its powers. FeSi is in space group $P2_13$ (T^4), a space group which is nonsymmorphic and contains 12 symmetry operations. The space group

operation involving C_3 are associated with primitive translations and the remaining operators in the tetrahedral point group T are associated with non-primitive translations [3]. In an 'ideal' B20 structure Fe and Si atoms lie in seven nearest neighbors of the other type. The neighboring atoms lie in 7 out of the 20 vertices of a regular pentagonal dodecahedron. In this 'ideal' B20 structure $u = -v = 1/4\tau$ = 0.15451, and the dodecahedron edge length is a/τ^2 where $\tau = (1+\sqrt{5})/2$ is the golden ratio. The experimental values of u and v differ from the 'ideal' values (experimentally, they are 0.1363(5) and $-0.1559(5)$, respectively), this leads to a splitting of the seven equivalent nearest-neighbor distances into three, three and one [8]. The driving force behind the stability of B20 cubic structure of the above mentioned monosilicides is still an open problem since no systematic study of the bonding in the B20, B1 and B2 phases has been made [8]. Vocaldo *et al*. [9] have suggested that the B20 phase is stabilized by the degree of covalency allowed by its atomic arrangement. Nuclear electric quardrupole and anisotropic magnetic dipole interactions exist in the cubic B20 structure of the transition-metal monosilicides since the point symmetry is less than cubic [2].

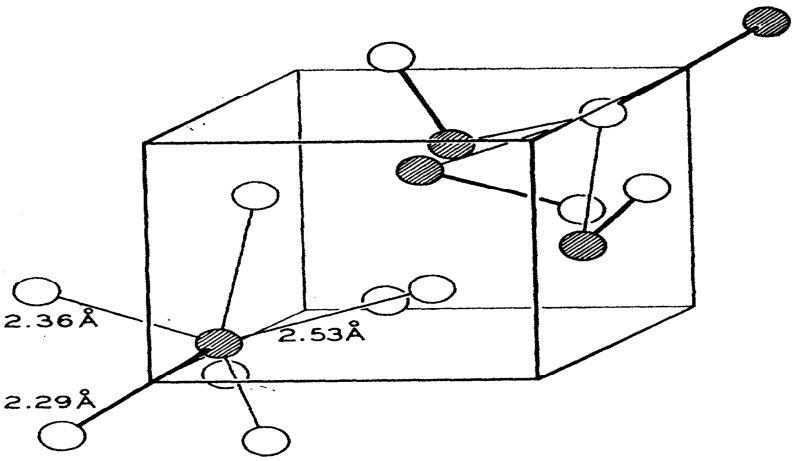

Fig 1.2: The FeSi structure. The Fe atoms, shown shaded have one Si neighbor in a [111] direction at 2.29 Å, three at 2.36 Å, and three at 2.53 Å [2].

2.3 FeSi as a kondo insulator

Kondo insulators are a group of materials with a nonmagnetic ground state characterized by extremely narrow charge-excitation gaps induced by strong electron correlations. Interaction of localized magnetic moments with the conduction electrons is defined as the Kondo effect. FeSi in particular may be strongly correlated in a similar class to the Kondo insulators [10]. FeSi is a paramagnetic metal in the high temperature region ($\geq$ 400 K) and its resistivity increases significantly with decreasing temperature below around 300 K. Concurrently the magnetic susceptibility decreases with decreasing temperature. Aeppli and Fisk concluded that the existence of such a nonmagnetic insulating state at low temperature is a characteristic of a Kondo insulator. It was also suggested that FeSi might represent the first example of a Kondo insulator involving weak hybridization of 3d electrons and a conduction band [11].

Inelastic-neutron scattering experiments reveal the picture of thermally induced spin fluctuations in FeSi similar to rare-earth compound CeNiSn, which is considered to be a Kondo insulator. Mason *et al.* [12] suggested that FeSi might represent the first example of transition metal which is a Kondo insulator. Interest in the study of other narrow-gap materials like $Ce_3Bi_4Pt_3$ and CeNiSn which is a class of strongly correlated insulators is gathering momentum. These materials have an insulating gap of order T_K (Kondo temperature). In contrast to the spin fluctuation picture, the Kondo insulator picture emphasizes on the character of the charge excitations at low temperature in that the system forms a nonmagnetic insulating state. The insulating state is ascribed to a coherent hybridization gap, where the couplings have been modified by strong correlations and are characterized by a Kondo temperature scale T_k [10]. Schlesinger et al. [13] measured infrared reflectivity of FeSi and observed an optical gap of 800K, which has diverted by 250K. Such kind of behavior is analogous to that seen in neutron measurements of $Ce_3Bi_4Pt_3$ and CeNiSn [14].

FeSi and some classes of Kondo insulators known as the rare earth intermetallics differ from Mott-Hubbard insulators, in that they are correctly predicted by band theory to be insulators without structural transition. However the extent to which these insulators are different from conventional insulators and semiconductors is unclear [15].

2.4: Magnetic properties of FeSi

2.4.1 Introduction

Magnetic semi-conductors are attracting great scientific interest because of their potential use for spintronics and as sensing elements in various sensor devices, as stress/force sensors (based on magnetoelastic responses), as magnetic labels (based on their bistable behavior) or as magnetic field sensors (based on their significant magnetoimpedance) [16]. Integrated circuits made of Semi-conductor used for information processing and communication devices generally take advantage of the charge of electrons, whereas magnetic materials used for recording information (hard disks, magnetic tapes, magnetic optical disks) make use of the electron spin. The mass, charge and spin of electrons are the cornerstone of the information technology (IT) we use today. If both the charge and spin of an electron could be harnessed simultaneously then the performance of electronic devices would be further enhanced.

Promising candidates for technological applications are the transition metal monosilicides and their alloys. FeSi displays novel magnetic properties that are temperature dependent and that justifies the sole reason why this compound has drawn so much attention over the last 60 years. FeSi is non-magnetic narrow-gap semi-conductor at low temperature and becomes paramagnetic metallic above 300 K. Evangelou *et al.* [17] has pointed out the possibility of ferromagnetic correlations in FeSi above 100 K. Alloys of transition metal monosilicides have been identified for technological applications; one of them is $Fe_{1-x}\,Co_x\,Si$. This material is remarkable in that the two end members (x = 0) and (x = 1) are both non-magnetic, it is magnetic for almost all intermediates compositions [18]. This compound has been of interest to many researchers because of its potential as a material for silicon-based spintronics applications where magnetic semi-conducting films could serve as injectors and collectors of spin-polarized currents in silicon transistors [19].

2.4.2: Theory on magnetic properties of FeSi

Interest in iron monosilicides started in the late 30's, when Foex discovered that the magnetic susceptibility of this compound increased with temperature above 200 K. Benoit later confirmed the results after observing the broad susceptibility χ (T) near 540 K. Benoit observed that at temperature T = 0 K FeSi becomes a non-magnetic insulator. At temperature T = 90 K the magnetic susceptibility decreases first and significantly increases showing a gradual transition from non-magnetic insulator to a paramagnetic metal with increasing temperature. Above 100 K, the magnetic susceptibility rises exponentially with increasing temperature passes through a maximum at approximately 540 K and obeys a Curie-Weiss type behavior at high temperatures whilst χ (T) will be decreasing. FeSi becomes metallic above 300 K.

It has been proposed through the general self-consistent renormalization theory of spin fluctuations that at temperatures above 100 K local magnetic moments of FeSi become thermally induced. Moreover, inelastic neutron scattering experiments have confirmed the presence thermally induced spin fluctuations in FeSi. At present there are only a few applications applicable for the interpretation of low temperature T < 70 K, Curie-Weiss like tale of the magnetic susceptibility and the absence of the magnetization saturation M (H,T = 4.2 K) in fields up to 200 KOe. Most common used explanation is said to be due to local fluctuations in the relative concentrations of Fe and Si in the FeSi structure play a very important role in the compound. Moreover residual imperfections in the crystal such as lattice defects, impurities, off-stoichiometry play a very important role as well. Another explanation is said to be due to Pauli paramagnetic contribution from the charge carriers in the narrow conduction band at Fermi level E_F and another explanation although unusual is attributed to the presence of paramagnetic impurity moments. A very weak ferromagnetic response has been detected at helium temperature and is said to be due to the presence of the uncompensated iron in the samples.

A number of different approaches have been suggested to try and explain the high temperature magnetic properties of FeSi. However the theoretical interpretation of these observations remains controversial. A first approach uses a theory of itinerant-electron magnetism where FeSi is described as a nearly ferromagnetic semiconductor; spin-fluctuations with strong temperature dependence amplitudes will strongly influence the thermal and magnetic properties of this compound. A second approach is based upon Kondo-lattice description whereby the high

temperature magnetism is thought to arise from localized magnetic moments of Fe, which are not Kondo compensated above a certain critical temperature, in this interpretation there is possible correlation of d- and f-electron systems. The high temperature magnetic behavior can also be attributed to thermally induced intermediate valence of Fe in FeSi. In this concept of intermediate valence, the ground state is claimed to be d^6Fe^{2+} hybridized with Si leading to spin zero S=0 (the orbital momentum is quenched) and the lowest excited state is d^7Fe^{1+} hybridized with Si with spin 3/2 [20].

Manyala *et al.* [19] revealed that the bulk and thin films of FeSi and its alloys displays different magnetic properties. Thin films of FeSi show ferromagnetism with significant magnetic hysteresis in contrast to the very weak paramagnetism of bulk FeSi. However Manyala *et al.* [19] could not explain the existence of ferromagnetism in thin films in contrast to weak paramagnetism in the bulk sample. Ferromagnetism in thin films is attributed to any of the four processes: spontaneous magnetization, domain structure, induced anisotropy and switching mechanism [21]. Further investigations are required to verify the exact cause of the transition from paramagnetism to ferromagnetism.

References

[1] Y. Onose, N. Takeshita, C. Terakura, H. Takagi, and Y. Tokura, Phys. Rev**. B72,** 224431 (2005)

[2] V. Jaccarino, G. Wertheim, J. Wernick, L. Walker, and S. Arajs, Phys. Rev.160, 3 (1967).

[3] L. Mattheiss and D. Hamann, Phys. Rev. B **47**, 13 114 (1993).

[4] H. Watanabe, H. Yamamoto, and K. Ito, J.Phys.Soc.Jpn. **18,** 995 (1963).

[5] D. van der Marel, A. Damascelli, K. Schulte, and A. Menovsky, Physica, B 244, 138-147 (1998).

[6] T. Jarlborg, Phys.Rev.**B59,** 23 (1999).

[7] Wood et al., J. Appl. Crystallogr., 29, 215-218 (1996).

[8] A. AI-Sharif, M. Abu-Jafar, and A. Qteish, J.Phys: Condens. Matter **13,** 2807-2815 (2001).

[9] L. Vocaldo, G. Price, and I. Wood, Acta Crystallogr. B **55,** 484 (1999).

[10] C. Fu, M. Krijn, and S. Doniach, Phys. Rev. **B49,** 3 (1994).

[11] G. Aeppli and Z. Fisk. Kondo insulators. Comments Condens. Matter Phys. **16**, 155-165 (1992).

[12] T. Mason, et al. Phys. Rev. Lett. **69,** 490 (1992).

[13] Z. Schlesinger et al., Phys. Rev. Lett. **71,** 1748 (1993).

[14] A. Severing et al., Phys. Rev. B **44,** 6832 (1991).

[15] J. DiTusa et al., Phys. Rev. B **58,** 16 (1998).

[16] M. Vazquez, J. Magn. Magn. Mat**.226-230**,693-699 (2001).

[17] S. Evangelou and D. Edwards, J. Phys. C **16,** 2121 (1983).

[18] N. Manyala, Y. Sidis, J.DiTusa, G. Aeppli, D. Young and Z. Fisk. Nature **404**,581-584 (2000).

[19] N.Manyala, B.Ngom, A.Beye, R.Bucher, M.Maaza, A. Strydom, A. Forbes, A. Johnson and J. DiTusa, Appl.Phys.Lett.**94**, 232503 (2009).

[20] N. Sluchanko et al., Phys. Rev. B 65, 064404 (2002).

[21] S.Chikazumi, Physics of Magnetism, J. Wiley and Sons, (1964).

CHAPTER 3: Electron spin resonance (ESR)

3.1: Introduction

Electron spin resonance (ESR) spectroscopy deals with the interaction of electromagnetic radiation with the intrinsic magnetic moment of electrons arising from their spin. This technique can probe magnetic properties (such as ferromagnetism) in substances with one or more unpaired electrons. In this section we want to demonstrate the effect of the DC static magnetic field (i.e. low-field or high field) on the spin state of unpaired electrons. We assume that at low field centred at B = 0, the separation between the upper energy state and lower energy state ΔE = 0 and in such the spins and magnetic moments of unpaired electrons are randomly oriented with equal energy.

3.2: Electron spin resonance (ESR) in the higher DC static field.

Electrons occurring in pairs have a net moment of zero and therefore cannot interact with electromagnetic radiation. The electric field ($\mathbf{E_1}$) and magnetic field ($\mathbf{B_1}$) components associated with electromagnetic radiation are perpendicular to each other and to the direction of propagation and oscillate at frequency ν. The energy of an electromagnetic radiation is given by $\varepsilon = h\nu$ [1]. Every electron possesses an intrinsic magnetic moment due to its spin. The spin has quantum number $s = \frac{1}{2}$, with magnetic components $M_S = \frac{1}{2}$ and $M_S = -\frac{1}{2}$

The magnetic moment of an electron spin $\mu_S = 2\beta S$ (3.2.1)

The magnetic moment associated with orbital momentum is $\mu_L = 2\beta L$ (3.2.2)

Bohr magneton is defined by $\beta = \frac{e\hbar}{2m}$ (3.2.3)

S = spin angular momentum operator and;

L = orbital momentum operator

The Bohr magneton β serve as a constant to convert the angular momentum to magnetic moment in electromagnetic c.g.s units.

In the presence of zero magnetic field the spins and magnetic moments of the unpaired electrons will be pointing randomly with equal energy. If a DC static magnetic field H_{DC} is applied across the sample, the electron's magnetic moment aligns itself either parallel ($M_S = -\frac{1}{2}$) or anti-parallel ($M_S = \frac{1}{2}$), precess around its axis and energy levels are shifted to achieve substantial measured splitting. Increasing DC static magnetic field H_{DC} will induce an electron to precess faster and acquire more kinetic energy.

Electrons will fall into groups with different energies i.e. those with their spins aligned parallel to the field will have an energy of $E = \frac{1}{2} g\beta H$ less than the zero-field value, and those with their spins aligned antiparallel to the field will have an energy of $E = \frac{1}{2} g\beta H$ greater than the zero field value. The parallel alignment corresponds to the lower energy state and the anti-parallel alignment corresponds to the higher energy state. The separation between the lower state and the upper state is given by $\Delta E = g\beta H = E_{+\frac{1}{2}} - E_{-\frac{1}{2}}$ (3.2.4)

Equation 5.2.6, implies that by increasing the DC static magnetic field H_{DC} the gap between $M_S = \frac{1}{2}$ and $M_S = -\frac{1}{2}$ energy states is widened as shown in figure1[2].

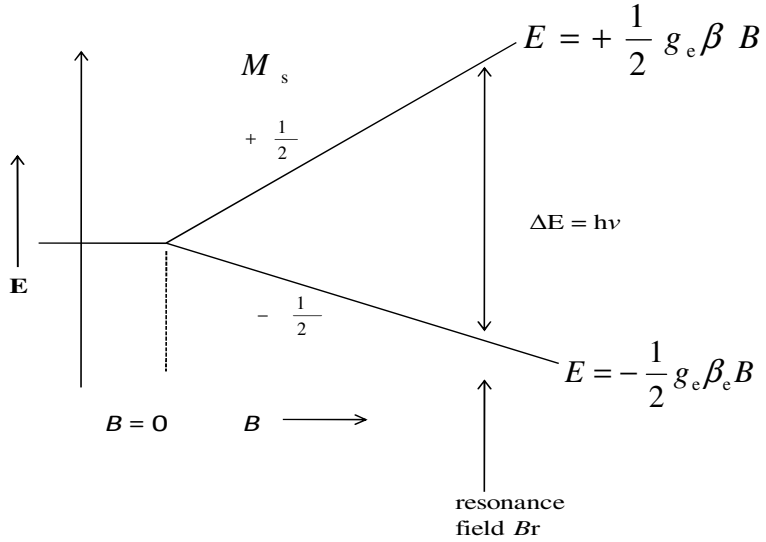

Fig. 1: *Energy level diagram for the simplest system (e.g.* free *electron) as a function of static magnetic field* ***B****, showing ESR absorption. E represents the energies of the* $M_S = \pm\frac{1}{2}$ *states and* M_S *for electron spins.*

An unpaired electron can move between the two energy levels by either absorbing or emitting electromagnetic radiation (microwave radiation) of energy $\varepsilon = h\nu$, such that resonance condition $\varepsilon = \Delta E$ is obeyed. For absorption to occur, two conditions must be fulfilled: (1) the energy $\varepsilon = h\nu$ of an electromagnetic wave must correspond to the separation between certain levels in a molecule, and (2) the oscillating electric-field component $\mathbf{E_1}$ must be able to interact with an oscillating electric- dipole (or higher) moment and similarly an oscillating magnetic component $\mathbf{B_1}$ of electromagnetic radiation must be able to interact with a molecule containing magnetic dipole moment [1].

3.3: Effect of temperature in electron spin resonance (ESR).

In our experiment we deal with a macroscopic sample which means a statistical ensemble of magnetic moments. Therefore, we need to consider the relative populations of the energy levels n_1 and n_2, which are given by the Boltzmann distribution. Assuming a system to be in thermal equilibrium implies that there will be more electrons in the ground state than in the upper state, and therefore there will be a net absorption of radiation of frequency ν.

Generally the distribution of electron between the two states is given by the Maxwell-Boltzmann expression;

$$\frac{n_1}{n_2} = e^{\frac{-\Delta E}{KT}} \qquad (3.3.1)$$

ΔE = separation between the two energy levels

K = Boltzmann constant

T = absolute temperature

n_1 and n_2 = electrons in the upper state and lower state respectively. It can be seen from equation (3.3.1) that the intensity of absorption can be increased by lowering the temperature since T is then reduced and the difference between n_1 and n_2 increased and hence net absorption occurs. At room temperature n_1 is far much greater than n_2 for a Zeeman splitting corresponding to a frequency of 10 GHz [2].

3.4: Electron spin resonance (ESR) in the low DC static field.

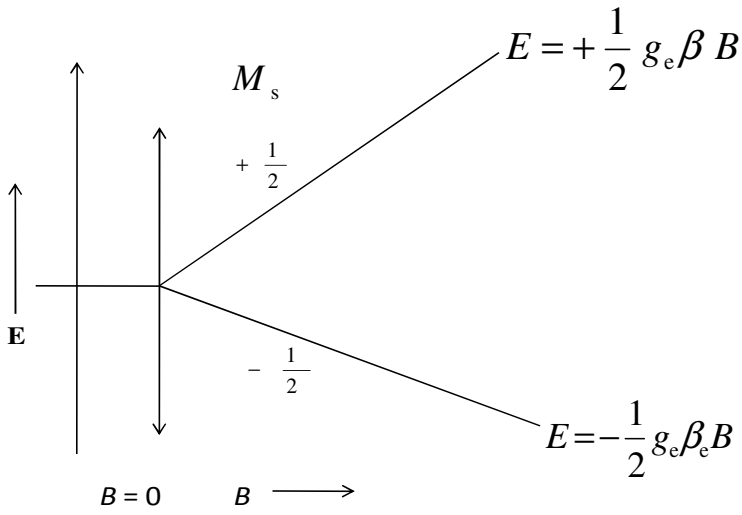

Fig. 2: Shows LFA centered at B = 0 as a non-resonant phenomenon.

The gap between energy states $M_s = \pm\frac{1}{2}$ does not match the energy of a microwave $\varepsilon = h\nu$ therefore the phenomena is non-resonant. Weaker energy is absorbed since energy of a microwave is strongly absorbed during resonance conditions $\Delta E = \varepsilon$. In the absence of the external magnetic field only the permanent dipole moments is expected to be interacting with the oscillating magnetic component $\mathbf{B_1}$ of electromagnetic radiation [1]. We assume that at low-field centered at B = 0, ΔE = 0.

3.5: Magnetization in a static magnetic field

In this section we investigate the effect of Magnetization M, to static magnetic field and to sinusoidally varying microwave field B_1. In the absence of external magnetic field the magnetization M if present is fixed in space, with components M_X, M_Y and M_Z in an arbitrary Cartesian coordinate system. When the magnetic moments are exposed to static and homogeneous field B, M precesses about B with Larmor frequency with the same sense as B_1.

Magnetic moments exposed to a static and homogeneous magnetic field, B in the absence of relaxation are said to be in dynamic equilibrium. Considering magnetization, M not fixed and moving according to the equation of motion of magnetization [1]. According to equation 3.5.1 the magnetization M will precess about the direction of B at a constant angle so long as B is a uniform, constant field. In practice, the magnetization M spirals into parallelism with the applied field B, due to damping effects [2].

$$\frac{dM}{dt} = \gamma_e M \times B \tag{3.5.1}$$

where γ_e is the electronic magnetogyric ratio $\gamma_e = \frac{gB_e}{\hbar}$.

Taking $\vec{B} = (0,0,B)$,

$$\begin{aligned}\left(\frac{dM_x}{dt}, \frac{dM_y}{dt}, \frac{dM_z}{dt}\right) &= \gamma_e M \times B \\ &= \gamma_e \left(M_x, M_y, M_z\right) \times \left(0,0,B_z\right) \\ &= \gamma_e \begin{vmatrix} i & j & k \\ M_x & M_y & M_z \\ 0 & 0 & B_z \end{vmatrix}\end{aligned} \tag{3.5.2}$$

$$\left(\frac{dM_x}{dt}, \frac{dM_y}{dt}, \frac{dM_z}{dt}\right) = \gamma_e \left[\left(M_y \times B_z\right) i - \left(M_x B_z\right) j + k\left(0\right)\right]$$

$$\frac{dM_x}{dt} = \gamma_e M_y B \tag{3.5.3}$$

$$\frac{dM_y}{dt} = -\gamma_e M_y B \tag{3.5.4}$$

$$\frac{dM_z}{dt} = 0 \tag{3.5.5}$$

With solutions

$$M_x = M_\perp^0 \cos \omega_B t \tag{3.5.6}$$

$$M_y = M_\perp^0 sin\ \omega_B t \tag{3.5.7}$$

$$M_z = M_z^0 \tag{3.5.8}$$

Equations (3.5 6), (3.5.7), (3.5. 8) reveal that M precess about B at a constant angle with Larmor frequency $(\omega_B = -\gamma_e B)$ if $M_\perp^0 \neq 0$.

Including relaxation effects, we have,

$$\frac{dM_x}{dt} = \gamma_e B M_y - \frac{M_x}{\tau_2} \tag{3.5.9}$$

$$\frac{dM_y}{dt} = \gamma_e B M_x - \frac{M_y}{\tau_2} \tag{3.5.10}$$

$$\frac{dM_z}{dt} = \frac{M_\perp^0 - M_z}{\tau_1} \tag{3.5.11}$$

where τ_1= longitudinal relaxation time.

and τ_2= transverse relaxation time.

After the addition of an AC microwave radiation we have;

A sinusoidally varying monochromatic field B_1 is imposed in a direction perpendicular to B. B_1 has components,

$$B_{1x} = B_1 \cos \omega t \tag{3.5.12}$$

$$B_{1y} = B_1 \sin \omega t \tag{3.5.13}$$

$$B_{1z} = 0 \tag{3.5.14}$$

$$\frac{dM}{dt} = \gamma_0 M \times B_1 \tag{3.5.15}$$

$$\left(\frac{dM_x}{dt}, \frac{dM_y}{dt}, \frac{dM_z}{dt}\right) = \gamma_0 \begin{vmatrix} i & j & k \\ M_x & M_y & M_z \\ B_{1x} & B_{1y} & B_{1z} \end{vmatrix}$$

$$= \gamma_0 \left[\left(M_y B_{1z} - M_z B_{1y}\right) - \left(M_x B_{1z} - M_z B_{1x}\right) + \left(M_x B_{1y} - M_y B_{1x}\right) \right]$$

$$\frac{dM_x}{dt} = \gamma_e \left(M_y B_{1z} - M_z B_{1y}\right) \tag{3.5.16}$$

$$\frac{dM_y}{dt} = -\gamma_e \left(M_x B_{1z} - M_z B_{1x}\right) \tag{3.5.17}$$

$$\frac{dM_z}{dt} = \left(M_x B_{1y} - M_y B_{1x}\right) \tag{3.5.18}$$

But $B_{1z} = 0$.

$$\frac{dM_x}{dt} = \gamma_e \left(-M_z B_{1y}\right) \tag{3.5.19}$$

$$\frac{dM_y}{dt} = \gamma_e \left(M_z B_{1x}\right) \tag{3.5.20}$$

$$\frac{dM_z}{dt} = \gamma_e \left(M_x B_{1y} - M_y B_{1x} \right) \tag{3.5.21}$$

Adding equation (3.5.9), (3.5.10) and (3.5.11) to (3.2.19), (3.2.20) and (3.2.21) respectively yields

$$\frac{dM_x}{dt} = \gamma_e \left(BM_y - B_{1y} \right) - \frac{M_x}{\tau_2} \tag{3.5.22}$$

$$\frac{dM_y}{dt} = \gamma_e \left(B_{1x} M_z - BM_x \right) - \frac{M_y}{\tau_2} \tag{3.5.23}$$

$$\frac{dM_z}{dt} = \gamma_e \left(B_{1y} M_x - B_{1x} M_y \right) - \frac{M_z^0 - M_z}{\tau_1} \tag{3.5.24}$$

Substituting for $B_{1x} = B_1 \cos \omega t$, $B_{1y} = B_1 \sin \omega t$ *and* $B_{1z} = 0$,

$$\frac{dM_x}{dt} = \gamma_e \left(BM_y - B_1 \sin \omega t \, M_z \right) - \frac{M_x}{\tau_2} \tag{3.5.25}$$

$$\frac{dM_y}{dt} = \gamma_e \left(B_1 \cos \omega t \, M_z - B M_x \right) - \frac{M_y}{\tau_2} \tag{3.5.26}$$

$$\frac{dM_z}{dt} = \gamma_e \left(B_1 \sin \omega t \, M_x - B_1 \cos \omega t \, M_y \right) - \frac{M_z^0 - M_z}{\tau_1} \tag{3.5.27}$$

In principle, one can integrate these equations to obtain the functional form of the components of M.

3.6: Spin dynamics

In this section we want to investigate the spin dynamics by focusing on the population difference of a two level spin system so as to prove that the population difference evolves exponentially as a function of time to its steady state value and hence M_Z evolves exponentially to its equilibrium value M_Z^0. The investigation will help us to understand the effect of increasing microwave power to the absorption phenomenon.

Given that N_u and N_l are the occupancy numbers of the upper and lower levels, the population difference is given by;

$$\Delta N = N_l - N_u \tag{3.6.1}$$

Total population N is given by,

$$N = N_l + N_u \tag{3.6.2}$$

Combining (3.6.1) and (3.6.2) gives,

$$N_u = \frac{1}{2}(N - \Delta N) \tag{3.6.3}$$

and

$$N_l = \frac{1}{2}(N + \Delta N) \tag{3.6.4}$$

From (3.6.1), defining the rate of spin per unit time, we get,

$$\frac{d\Delta N}{dt} = \frac{dN_i}{dt} - \frac{dN_u}{dt} \tag{3.6.5}$$

Let $Z\downarrow$ be the probability of electron per unit time from the upper level to the lower level and $Z\uparrow$ the probability of electron spin per unit time from lower level to upper level.

$$Z\downarrow = \frac{e_u}{N_u} \qquad \Rightarrow e_u = N_u Z\downarrow$$

Similarly $e_l = N_l Z\uparrow$

$$\frac{d\Delta N}{dt} = 2e_l - 2e_u = 2N_l Z\uparrow - 2N_u Z\downarrow$$

Thus

$$\frac{d\Delta N}{dt} = 2N_l Z\uparrow - 2N_u Z\downarrow \tag{3.6.6}$$

The factor 2 appears because an upward or downward transition changes ΔN by 2.

$$\begin{aligned}\frac{d\Delta N}{dt} &= N\left(Z\downarrow - Z\uparrow\right) - \Delta N\left(Z\downarrow + Z\uparrow\right)\\ &= \left(\frac{NZ\downarrow - Z\uparrow}{Z\downarrow + Z\uparrow} - \Delta N\right)\left(Z\downarrow + Z\uparrow\right)\end{aligned} \tag{3.6.7}$$

The spin system approaches a steady state represented by ss, hence

$$\begin{aligned}&\frac{d\Delta N}{dt} = 0\\ &\Rightarrow \Delta N^{ss} = N_l^{ss} - N_u^{ss}\end{aligned} \tag{3.6.8}$$

Thus

$$\Delta N^{ss} = \frac{NZ\downarrow - Z\uparrow}{Z\downarrow + Z\uparrow} \tag{3.6.9}$$

and

$$\frac{d\Delta N}{dt} = \left(\Delta N^{ss} - \Delta N\right)\left(Z\downarrow + Z\uparrow\right) \tag{3.6.10}$$

The quantity $\left(Z\downarrow + Z\uparrow\right)^{-1}$ is the relaxation time τ_1

$$\frac{d\Delta N}{dt} = \frac{\Delta N^{ss} - \Delta N}{\tau_1} \tag{3.6.11}$$

This has a solution,

$$\Delta N = (\Delta N)_0 + \left[\Delta N^{ss} - (\Delta N)_0\right]\left\{1 - \exp\left[-(t - t_0)/\tau_1\right]\right\} \tag{3.6.12}$$

Thus $\Delta N(t)$ evolves exponentially from ΔN_0 toward ΔN^{SS} with a rate constant $k_1 = \tau_1^{-1}$ where τ_1 is now seen to be the time required for ΔN to change by $\left[\Delta N^{ss} - (\Delta N)_0\right]\left[1 - e^{-1}\right]$. Since the component M_Z along B of the magnetization M is proportional ΔN [i.e. proportional to $\left(\frac{g\beta_e}{2V}\right)\Delta N$ for non interacting unpaired electrons in a volume V], M_Z also evolves exponentially to its equilibrium value M_Z^0 [1].

3.7: Low-field microwave absorption (LFA) phenomena

3.7.1: Introduction

Microwave power absorption (MPA) centered at zero magnetic field (B = 0), termed low-field microwave absorption (LFA) has been observed in various materials: high temperature superconductors, ferrites, manganites, semiconductors, doped silicate glasses and in soft magnetic materials. Several authors have shown a strong correlation between (LFA) and giant magnetoimpedance (GMI) phenomenon mostly in Co-based amorphous ribbons. The GMI effect can be harnessed for several technological applications. GMI sensors offer superior advantages such as low power consumption, small size and better thermal stabilities over conventional magnetic sensors.

3.7.2: Correlation between low-field microwave power absorption (LFA) and magneto-impedance (MI).

Considering a microwave with both electric (E) and magnetic (H) fields. The time average density of power absorption (P) for a ferromagnetic conductor can be expressed by a complex Poynting vector as [3]

$$P = \frac{1}{2} Re\,[\,E \times H^{*}\,] \qquad (3.7.2.1)$$

H^{*} is a complex conjugate of H and Re [x] is the real part of the operator.

The AC surface impedance for a ferromagnetic conductor is defined as the ratio of the fields at the surface given by:

$$Z_s = \frac{E_s}{H_s} \qquad (3.7.2.2)$$

$$E_s = H_s Z_s \tag{3.7.2.3}$$

$$E_s \times H_s = E_s H_s \sin \emptyset \tag{3.7.2.4}$$

But $E_s \perp H_s$ $$E_s \times H_s = E_s H_s \sin 90^{\circ} \tag{3.7.2.5}$$

$$E_s \times H_s = E_s H_s \tag{3.7.2.6}$$

Substituting equation (3.7.2.6) into equation (3.7.2.1) we have:

$$P = \frac{1}{2} Re\,[\,E_s \times H_s\,] = \frac{1}{2} Re\,[\,E_s H_s\,] \tag{3.7.2.7}$$

Now substituting equation (3.7.2.3) into equation (3.7.2.7) for E_s we have:

$$P = \frac{1}{2} Re\,[Z_s H_s H_s\,] = \frac{1}{2} H_s^2 Re\,(Z_s) \tag{3.7.2.8}$$

Then the time-average density of the microwave power absorption can be written as:

$$P = \frac{1}{2} H_s^2 Re\,(Z_s) \tag{3.7.2.9}$$

The AC magnetic field H_s, in a ferromagnetic conductor at high frequency is generated by a uniform current $j = \delta E_s$ (with δ the electrical conductivity) induced by the AC electric field E_s; and therefore H_s is constant to changes of an applied static magnetic field

We can therefore establish a relation between the field derivative $\left({}^{dP}/_{dH}\right)$ of the microwave power absorption and the rate of change of $Re\,(Z_s)$ with an applied static magnetic field H given as:

$$\frac{dP}{dH} = \frac{H_s^2}{2} \frac{dRe(Z_s)}{dH} \tag{3.7.2.10}$$

The magneto-impedance (MI) is defined as the change of the impedance of a magnetic conductor subjection to excitation current under the application of the static magnetic DC field H_{DC}. It is very similar phenomenon to low-field microwave absorption (LFA) as it is controlled by anisotropy field. In the quasi-static regime, magneto-impedance (MI) is controlled by low frequency magnetization process. At higher frequency the ferromagnetic resonance (FMR) dominates the MI behavior [4]. Giant magnetoimpedance (GMI) extends over a wide frequency range from few K Hz, where the dominant magnetization process is domain wall movements to G Hz range where only spin dynamics can follow the AC microwave field [5].

3.7.3: Low-field microwave power absorption (LFA) in different materials.

Microwave power absorption (MPA) or low-field microwave absorption centered at zero magnetic field has been observed in a wide variety of materials: high temperature superconductors, ferrites, silicate glasses, and semiconductors [5, 6]. For high temperature superconductors the emergence of this absorption has been widely accepted as a signature of the superconductive state. This signal is reflecting the dissipative dynamics of the fluxons characteristic of a mixed state. For ferrites this low field absorption signal is due to microwave absorption processes closely related to low-field magnetization processes of the sample and strongly depends on the anisotropy field such as in magneto-impedance (MI). For semi-conductors this signal is due to magneto-resistive effects. For manganites the appearance of low-field absorption signal (LFA) is used to indicate the onset of the ferromagnetic phase and provides a sensitive detector of ferromagnetism. For doped silicate glasses this low-field absorption signal is due to magneto-induced microwave conductivity in the dielectric glass which derives from spin-dependent charge migration within the first co-ordination sphere of the paramagnetic ion [6]. Low-field absorption signal has been reported recently in other soft magnetic materials as wires and thin films and have been interpreted as due to low-field spin magnetization processes [5]. Several authors have recently shown, however that ferro and ferrimagnetic materials can absorb microwave fields at low applied field i.e. magnetic field well below anisotropy field (H_k) [7]. Ferromagnetic materials exhibit a wide variety of behaviors

when subjected to A.C magnetic fields such as domain wall relaxation (DWR), magneto-impedance (MI) and ferromagnetic resonance (FMR) [6].

Low-field microwave absorption is associated with magnetization processes from the unmagnetized state ($H_{DC}=0$) to the saturated condition in many aspect similar to giant magneto-impedance (GMI) and clearly different from ferromagnetic resonance (FMR). The low field absorption signal (LFA) signal exhibits different characteristics such as hysteresis, and a minimum in power absorption at zero magnetic field. Hysteresis effect in the low-field absorption LFA shows that it is effectively a non-resonant phenomenon physically similar to giant magneto-impedance (GMI) [7].

3.7.4: Low-field microwave absorption signal (LFA) as a non resonant phenomenon.

The ${}^{dP}/_{dH}$ against H_{DC} centered about $H_{DC}=0$ signifies low-field absorption (LFA). The higher field has a resonant character and is associated with ferromagnetic resonance (FMR). The enlargement of the plot close to $H_{DC}=0$, if non-resonant shows magnetic hysteresis. The presence of hysteresis signifies non-Larmor dependence on dc field and according to Montiel *et al* [5] the hysteresis effect of LFA appears to be due to nonuniform surface magnetization processes. Larmor relationship implies: $\omega=\gamma H_{DC}$ where ώ is the resonance frequency, γ is gyromagnetic ratio and H is the total internal field upon spin and is associated with ferromagnetic resonance FMR [8].

3.7.5: Ferromagnetic resonance (FMR).

Low field absorption usually originates from the magnetization processes far from the saturation state and very similar to that of giant magneto-impedance (GMI), while ferromagnetic signal is due to absorption in the full saturation state and corresponds to the quantum-mechanical resonant

phenomenon. Ferromagnetic resonance (FMR) signal occurs at higher fields absorption unlike low-field microwave absorption (LFA) which occurs at lower fields [7].

Ferromagnetic resonance is the absorption, P, of microwave magnetic field by a ferromagnetic material, measured as a function of the applied DC magnetic field, H. If the magnetic field is modulated at an audio frequency, the derivative of the absorption $^{dP}/_{dH}$ is measured instead of the absorption itself [9]. FMR phenomena must satisfy the exact Larmor equation usually for frequencies in the GHz range.

In the case of a thin sheet with negligible anisotropy field within the sheet plane [10],

$$\omega = \gamma\,[BH_{dc}]^{1/2} \qquad (3.7.5.1)$$

Where ω is the microwave angular frequency (9.4 GHz), γ is the gyromagnetic ratio, H_{dc} is the static magnetic field and B is the magnetic induction of the sample ($B = H_{DC} + 4\pi M_S$); M_S is the saturation magnetization.

By assuming a spin-only behavior (Lande factor g = 2.0023) this therefore implies that γ is given by:

$$\gamma = \frac{e}{m_e} \qquad (3.7.5.2)$$

Where e and m_e are charge and mass of an electron respectively:

$\gamma = 1.76 \times 10^7$ rad / s / G for spin-only behavior

$\gamma = 1.76 \times 10^{11}$ rad / s / T for spin-only behavior

For the dc field normal to the plane of the sample the Larmor ferromagnetic resonance (FMR) condition is written as [11]:

$$\omega = \gamma\,[\,BH_{dc} - 4\pi M_s] \qquad (3.7.5.3)$$

3.7.6: Angular dependence of low-field microwave absorption (LFA).

LFA spectra is angular dependent, i.e. the width ΔH_{LFA} (where ΔH_{LFA} is the separation between the maxima and minima) and the intensity of this signal. The intensity of the signal decreases when increasing the angle up to 90° and the width increases for angle variations of 0° to 90°. As θ increases from 0° to 90°, the sample's plane turns from the parallel orientation, to the perpendicular orientation to the DC static magnetic field H_{DC}. Ferromagnetic resonance (FMR) and low-field absorption (LFA) are both modulated by total anisotropy field, including shape anisotropy field (SAF) and intrinsic anisotropy field (IAF). At 0° shape anisotropy field (SAF) is negligible and becomes maximum at 90°. The orientation of the AC field propagation to the sample affects the response of absorption. The propagation is more complex when AC field is perpendicular to the plane of the sample than when it is parallel to the plane of the sample. If the AC microwave field is perpendicular to the plane of the sample, shape anisotropy field (SAF) is minimized but not eliminated [4]. SAF corresponds to the energy needed to orientate the magnetic moment in the hardest direction, out of the plane. IAF corresponds to the energy needed to orientate the magnetic moment in the easiest direction, within the plane [12].

3.7.7: Changes in the permeability and skin depth of a material contributing to magneto-impedance (MI) and low-field microwave absorption (LFA).

Magneto-impedance (MI) is caused by the dependence of the penetration depth of the electromagnetic field on the permeability of the material, which varies at low fields due to magnetization processes [13]. The thickness of our films was 200 nm which is less than 1 μm and therefore it was necessary to work at higher frequencies. The high sensitivity of the MI on the DC applied field H_{DC} has attracted a great deal of attention because its potential applications in low cost field sensing [14]. The magnitude of the MI effects depends on the effective differential permeability of a material and its interplay with the thickness and frequency through the phenomenon called skin depth effect. Changing the relative angle ϑ between the film surface and the static DC field H_{DC} alters the dependence of the penetration depth of the microwave

radiation on the permeability and skin depth of the material and hence thus defines magneto-impedance (MI) of the material. Skin depth is given by the following formula

$$\delta_m = \sqrt{\frac{\rho}{\pi f \mu_{eff}}} \tag{3.7.7.1}$$

In the above expression, δ_m is the skin depth, ρ is the material's resistivity, $\mu_{eff} = \mu_{eff}(H, I_0, f)$ is the effective differential permeability, and I_0 and f are the amplitude and the frequency of the sinusoidal driving current, respectively. For stripes of a soft magnetic material, the impedance (Z) can be written as

$$Z \, \alpha \, \sqrt{\rho f \mu_{eff}} \tag{3.7.7.2}$$

This simplified expression clearly shows that the frequency of the probe current and the field dependence of the differential effective permeability define magneto-impedance (MI) and hence low-field microwave absorption (LFA).

3.7.8: Factors influencing low-field microwave absorption (LFA) of a material

A ferromagnetic conducting system can absorb microwave radiation with an efficiency that depends on parameters outlined below such as the;

- Magnetic domain structure
- Magnetic anisotropy
- The orientation of the incident propagation vector radiation i.e. whether the AC microwave field is oriented parallel or normal to the surface of the material influences the shape of the LFA spectra
- The orientation of the AC microwave field to DC field, whether they are parallel or perpendicular to each other, however the usual ESR geometry is AC microwave field normal to the DC field

- Conductivity of the material to be probed, in our case FeSi is a conductor of current
- Frequency of the AC microwave probe current
- Amplitude of the AC microwave probe current.

Absorption can easily be modified by static magnetic DC field H_{DC} , which changes the magnetic susceptibility, the penetration depth, the magnetization vector, the domain structure and spin dynamics. Such changes result in hysteresis. Cycling the field enables different irreversible domain configurations to occur and therefore a hysteresis effect can occur. Magneto-impedance (MI) and low-field microwave absorption (LFA) can therefore be understood as the absorption of electromagnetic radiation by spin systems that are modified by domain configurations and strongly depend on the anisotropy field. MI and LFA can be explained with classical electromagnetic processes, excluding quantum processes involved [5].

References

[1] J. Weil and J. Bolton, Electron Paramagnetic Resonance, second edition. J. Wiley, USA, (2007).

[2] J. Anderson, Magnetism and Magnetic materials, Chapman and Hall, London, (1968).

[3] J. Jackson, Classical Electrodynamics, second edition., John Wiley, USA, 1975.

[4] H. Montiel, G. Alvarez, R. Zamorano, and R.Valenzuela, J. Non-Cryst.Solids **353, 908**-910 (2007).

[5] H. Montiel, G. Alvarez, I. Betancourt, R. Zamorano, and R.Valenzuela, Appl. Phys. Lett. **86**, 072503 (2005).

[6] H. Montiel, G. Alvarez, I. Betancourt, R. Zamorano, R.Valenzuela, and R. Zamorano, Superficies y Vacio **19,** 3 (2006).

[7] R.Valenzuela, H. Montiel, G. Alvarez, and R. Zamorano, Phys.Status Solidi. **206,** 652-655 (2009).

[8] M. Vazquez, G. Badidni-Confalonieri and J. Torrejon et al.; "Low-field microwave

[9] H. Garcia-Miquel, and G. Kurlyandskaya, Chinese. Phys. **17**, 4 (2008).

[10] C. Kittel, Phys. Rev. **73,** 155 (1948).

[11] A. Morrish, The physical Principles of Magnetism, (John Wiley & Sons Inc., New York, (1965).

[12] G. Alvarez, H. Montiel, D. de Cos, A. Garcia-Arribas, R. Zamorano, J. Barandiaran, and R. Valenzuela, J. Non-Cryst.Solids **354,** 5195-5197 (2008).

[13] M. Knobel, L. Kraus, M. Vazquez, in : K. Buschow (Ed.), Handbook of Magnetic Materials, vol. 15, Elsevier, Amsterdam, 497-563 (2003).

[14] L. Panina, K. Mohri, T. Uchiyama, and M. Noda, IEE Trans. Magn. **31**, 1249 (1995).

CHAPTER 4: Experimental Techniques

4.1: Electric arc furnace

High purity Fe (99.999%) and Si (99.999%) were combined in the ratio of 50%-50% by an electric arc furnace in an argon atmosphere. The resulting mixture was polycrystalline FeSi bulk sample.

4.2: Annealing

Resulting FeSi bulk sample was annealed for 24 hours at 1000°C using evacuated quartz ampoules to improve homogeneity. The resulting FeSi bulk sample was crushed into powder and (Cu-Kα) x-ray diffraction (XRD) patterns were collected using an AXS Bruker diffractometer equipped with a position sensitive detector to determine the cubic B20 crystalline structure.

4.3: Pulse Laser Deposition (PLD)

Synthesis of polycrystalline FeSi, thin films was employed by using pulse laser deposition (PLD) techniques. Success in synthesizing crystalline films was attributed to the careful attention paid to pulse laser deposition PLD parameters such as deposition flux, laser fluence, laser energy, and ionization degree of the ablated material. Films were deposited on Si (111) substrates held 450^{0}C in vacuum (10^{-6} Torr). Substrate was cleaned ultrasonically with several organic solvents as well as with de-ionized water, etched in 20% HF solution and left in air for a period of between 2 and 30 days prior to deposition. An excimer laser wavelength of 248 nm, fluence of 4 J/cm^2 repetition rate of 10 Hz and 30 ns pulse duration was directed to arc melted FeSi targets for between 5 and 30 minutes. FeSi target material undergoes laser-solid interaction process which included excitation, ionization, ablation, melting and evaporation of the target

material. Plasma was generated near the surface of the target. The plasma expanded perpendicularly to the target surface and a flame called flume was formed. The evaporated species were contained in a forward ejected flume which includes neutral atoms, ions, molecules, electrons, cluster, and even small pieces of target materials. These species reached the substrate with high kinetic energy and were deposited on the substrate surface of Si (111). As the deposition was repeated, a thin film of FeSi of thickness 200 nm was formed on the substrate surface.

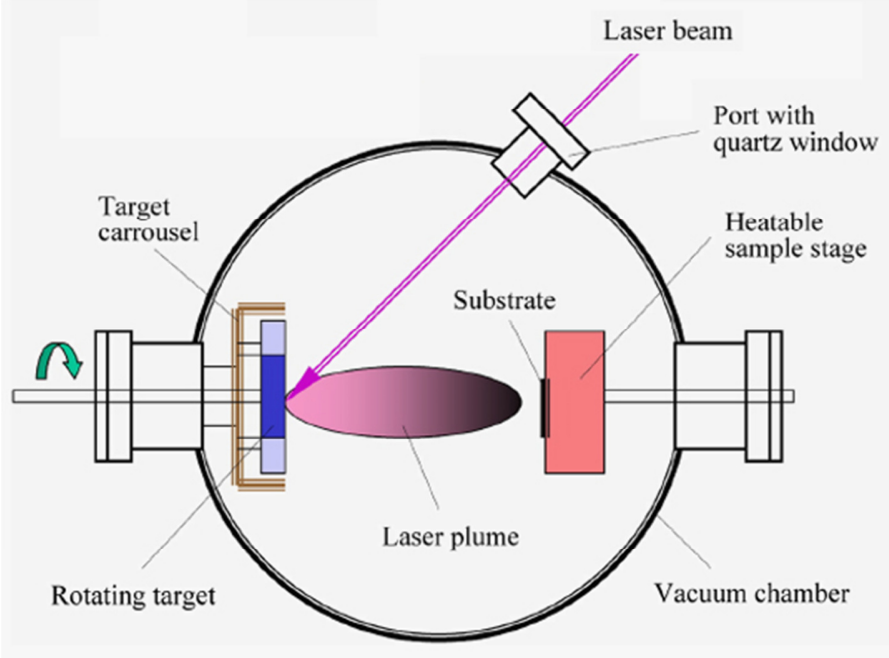

Fig. 6.3.1: illustrates the basic pulse laser deposition (PLD) set-up [1].

4.4: Characterization of FeSi sample.

The surface morphology of the sample was characterized using scanning electron microscopy (SEM) and atomic force microscopy (AFM). Transmission electron microscopy (TEM) probed the cross-sectional microstructure of the films. Film stoichiometry was determined by Rutherford backscattering spectroscopy (RBS) and energy dispersive spectrometry (EDS). TEM, and x-ray fluorescence SEM (EDX), reconciled with the concentrations of the starting materials. X-ray diffraction, transmission electron, and atomic force reveal films to be dense,

very smooth, and single phase with a cubic B20 crystal structure. Synthesis of single phase FeSi is challenging due to complex phase diagram of Fe and Si which is known to have five bulk phases [2].

4.5: Low-field microwave absorption (LFA) properties of FeSi thin films

Low-field microwave absorption (LFA) measurements at 9.4 GHz (X-band) were carried out on polycrystalline FeSi thin films using (JEOL-ESR) electron spin resonance spectrometer. The set-up of the electron resonance spectrometer (ESR) is shown in fig. 4.5.1 below.

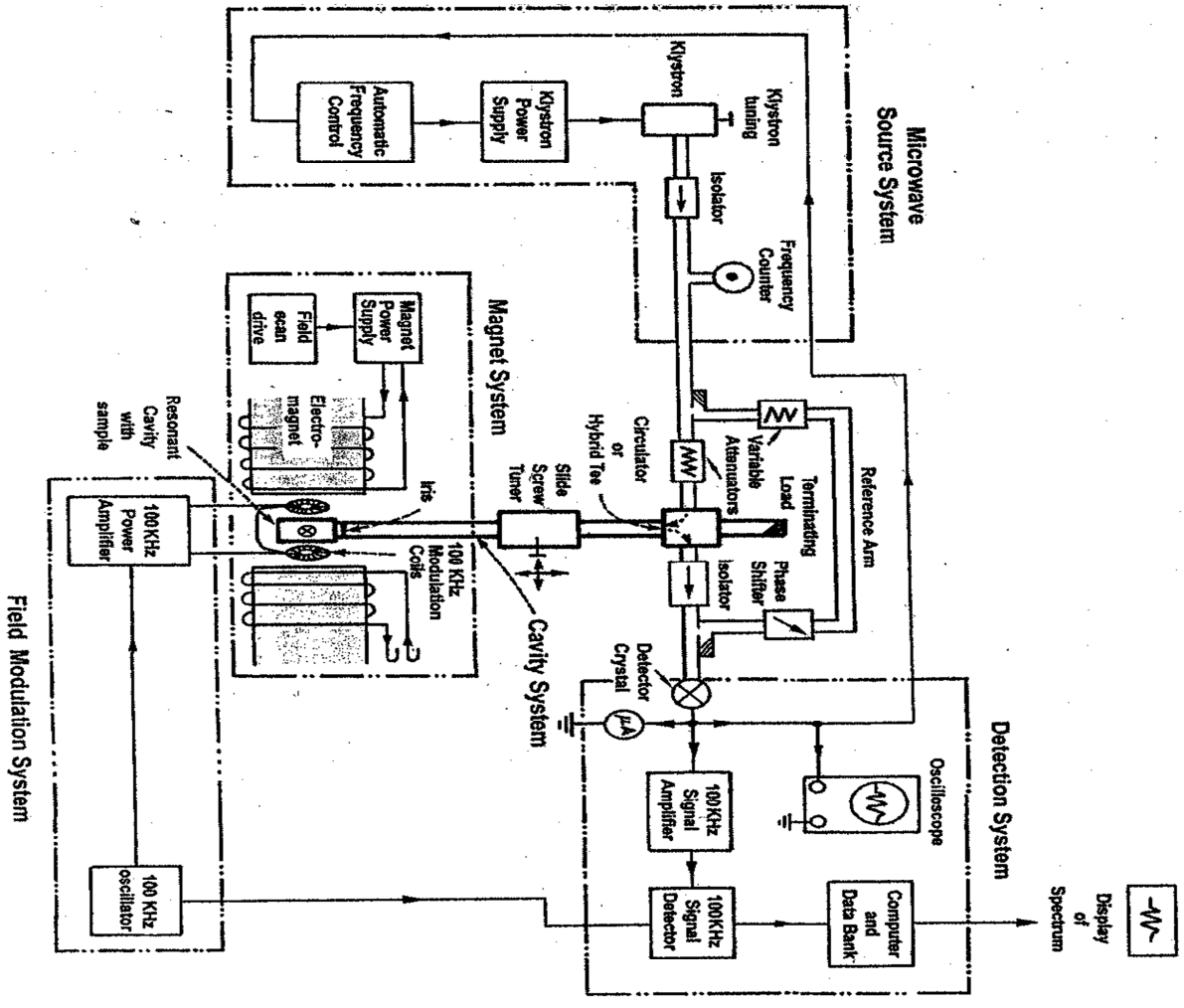

Fig. 4.5.1: Block diagram of ESR spectrometer system used at CSIR [3].

The low-field microwave absorption (LFA) properties of the thin films of FeSi were measured with modulation of a superimposed magnetic-field. The modulation field at a frequency of 100 KHz is applied parallel to the DC static magnetic-field and microwave signal is detected synchronously with the modulation using a phase sensitive detection. The low-field microwave absorption properties of the thin films of FeSi was investigated as a function of DC modulation field between 0.1 mT and 0.6 mT, temperature between 293K and 370 K, microwave power between 3 mW and 20 mW and angle between $\theta = 0^{\circ}$ and $\theta = 90^{\circ}$. The film surface was orientated parallel to both the DC static magnetic field and AC microwave field. The AC microwave field was propagated in a usual ESR geometry, DC static magnetic perpendicular to field.

A computer is incorporated in the electron spin resonance (ESR) spectrometer system. A Windows NT based user interface is adopted to allow performance in all operations using the keyboard and the mouse. Parameters that were adjusted by the computer include the DC modulation field and microwave power. The sample was rotated whilst inside the cavity to a precise angular position by the goniometer. The sample was rotated by an amount indicated on the calibration. At angle $\theta = 0^{\circ}$ the DC static magnetic-field was parallel to the film surface and at angle $\theta = 90^{\circ}$ becomes normal to the film surface. For angular variation from $\theta = 0^{\circ}$ to $\theta = 90^{\circ}$ the AC microwave field remains parallel to the film surface. Temperature was varied by making use of a digital temperature controller and the gas flow meter. The digital temperature controller controls the coil current so as to maintain desired temperature. The gas flow meter controls the amount of nitrogen gas flowing through the coil in the bottom of cavity dewar, implying that the nitrogen gas was heated as it passes through the coil. The amount of nitrogen gas flowing was controlled by a valve incorporated to the gas flow meter.

4.6: ESR experimental set up

The ESR spectrometer is an analytical instrument utilizing the phenomenon of magnetic resonance of electrons. It measures the absorption of microwave radiation corresponding to the energy splitting of unpaired electron when it is placed in a strong DC static field. The ESR

system consists of a microwave source system, cavity resonator, magnetic system and the detection system (i.e. spectrometer). ESR determines magnetic properties of different compounds with unpaired electrons. Any sample that contains unpaired electrons can, in principle, yield an electron spin resonance (ESR) spectrum.

In order to perform an ESR experiment one has to have a compound with one or more unpaired electrons. The FeSi thin film was set at the centre of the cavity resonator to avoid a phenomenon called leaking. The cavity incorporated is a closed cylindrical metallic box with an iris to allow the microwave to couple in and out. This cylindrical cavity operates in the TE_{011} mode. The dimensions of this cavity were matched to the wavelength of the microwaves so that the sample is held in a region where the magnetic field component of the radiation is maximized and the electric field is minimized. The shape and microwave characteristics of the film were taken into consideration. FeSi is a solid sample with relatively low dielectric losses; this will allow the measurements to be performed using standard ESR tube.

The region labeled microwave source system as illustrated in figure 4.5.1 contains components that produce the electromagnetic waves oscillating in the microwave region 9.4 GHz. Klystron produces coherent electromagnetic wave. The ESR spectrometer was equipped with an automatic tuning function. The instrument can automatically adjust the microwave frequency, coupling and phase to the optimum conditions. The klystron frequency was very stable so as to minimize fluctuations of the klystron temperature or of applied voltages and mechanical vibrations.

Three important components were involved in transmission of the microwave source power output to the resonator holding the thin film sample. These are the isolator, the attenuator and the circulator. An isolator was used to minimize perturbations of microwave source frequency due to significant backward reflections of microwave energy from the rest of the system. An isolator is a non-reciprocal implying that it exhibits properties that are not identical for waves travelling in the forward and in the reverse direction. It readily allows microwave in the forward direction while it strongly attenuates any reflections back to the microwave source. A circulator is a non-reciprocal device like the isolator. It serves to direct the microwave power to the cavity with the thin film sample and simultaneously to direct the power reflected from the cavity to the detector. The operation is a four port circulator. The attenuator controls the level of the

microwave power incident on the sample since it contains an absorptive element. The reference arm takes microwave power from the waveguide ahead of the circulator and restores it with adjusted power level and in phase after the circulator and resonator. The reference arm also ensures whether the absorption or dispersion signal from the spin system is detected.

The source of the static magnetic field is the electromagnet. The static magnetic field causes desires splitting of the spin energy levels. The magnetic system provides a stable, homogeneous magnetic field (H_{DC}) that is linearly variable within the desired range. The magnetic field was stable and uniform over the sample volume; field variations were kept within $\pm 1\mu T$ to resolve very narrow electron spin resonance (ESR) lines and to obtain the correct line shape. The polarity of the electromagnet is generally of less significance. The DC static field was oriented normal to the excitation field B_1 (i.e. the AC microwave field) at the sample. Stability was achieved by energizing the magnet with stable regulated power supply. The current should be extremely stable in order to avoid spurious noise that could interfere with the measurement. Hall probe measures the static magnetic field. Principle of operation is based on the Hall effect. The probe should be positioned vertically relative to the magnetic field in order to get maximum sensitivity. The probe is thermostated or temperature-compensated to avoid drift with changing probe temperature. Feedback systems adjust the magnet current to maintain fixed Hall-probe voltage. The Gauss meter converts the volt measured from the Hall probe into a value of magnetic field.

When the magnetic field is swept so as to achieve the resonance condition, electromagnetic radiation is absorbed by the sample leading to a small decrease in radiation intensity as noted by the detector. Since it is more efficient to detect an AC signal in the presence of a large .DC background and hence 100 KHz (H_{AC}) field is superimposed in the DC field. 100 KHz (H_{AC}) field is achieved by means of Helmholtz coils embedded in the walls of the cavity along the axis of the static field. A lock in detection is used to enhance signal sensitivity. This generates a signal that looks like the first derivative of the absorption line. In the detection system the amplified electron spin resonance signal (ESR) is mixed with the output of the field modulating 100 KHz oscillator. If the two signals are opposite in phase, the output from the system is minimum but however if they are exactly in phase the output is a maximum. A phase shifter

allows optimization of the output. The combined signal is rectified, filtered and recorded. The output signal depends strongly on the amplitude, phase of the signal and reference voltages. The modulation and detection system was monitoring, amplifying and recording the signal.

4.7: Data acquisition

A crystal diode is responsible for the detection and amplification of the spectra signal. The crystal rectifier diode consists of semi-conducting material. The incident microwave power causes the current to flow. The current I increases with microwave power and the sensitivity of the detection depends strongly on the slope dI/dP which is specific to each diode. After the detection and amplification by crystal rectifier diode, the electron spin resonance (ESR) spectra is converted to digital by an analog-to-digital converter and stored temporarily on digital oscilloscope before being transferred to the computer's memory. After the data was transferred to the computer memory, a laser printer was used to record spectra and the storage of data was done by a hard disk or a CD-R.

4.8: Sensitivity of the ESR spectrometer

Sensitivity or the minimum number of spins $N_{\min}$ detected by the machine depends upon photon frequency ν according to following equation [4].

$$N_{\min} = \frac{k_1 V}{Q_0 k_f \nu^2 P^{1/2}} \tag{4.8.1}$$

Where k_1 is a constant, V is the sample's volume, Q_O is the unloaded quality factor of the microwave cavity, k_f is the cavity filling coefficient, and P is the microwave power in the spectrometer cavity. In our case the ESR spectrometer was having sensitivity of 7×10^9 spins / 0.1 mT at a maximum output of 200 mW with 100 KHz magnetic-field modulation.

References

[1] http://www.physandtech.net/ Pulse laser deposition.

[2] N.Manyala, B.Ngom, A.Beye, R.Bucher, M.Maaza, A. Strydom, A. Forbes, A. Johnson and J. DiTusa, Appl.Phys.Lett.**94**, 232503 (2009).

[3] J.Weil and J. Bolton, Electron Paramagnetic Resonance, second edition. J. Wiley, USA, (2007).

[4] D. Ingram, Free radicals as studied by Electron Spin Resonance, Butterworths, London, (1958).

CHAPTER 5: Results and Discussions

5.1: Angular, microwave power, and temperature dependence of LFA measurements.

Low-field microwave absorption (LFA) measurements at 9.4 GHz (X-band) was investigated on pulse laser deposited (PLD) polycrystalline B20 cubic structure thin films grown on Si(111) substrate using electron spin resonance spectrometer (ESR). The films used in this study were well characterized using various microscopies [1]. The LFA properties of films were investigated as a function of DC-field modulation, temperature, microwave power and the orientation of DC-field with respect to film surface. The film was rotated from $\vartheta = 0^{\circ}$ (H_{DC} parallel to film surface) to $\vartheta = 90^{\circ}$ (H_{DC} normal to film surface) while the microwave magnetic field was kept parallel to the film surface. Such measurements were done to determine the angular dependence of LFA so as to verify effects of anisotropy field on the LFA shape. Temperature measurements were varied from T = 293 K to T = 400 K and the LFA signal strength was seen to be decreasing with increase in temperature. Such measurements were done to verify if the long range order would disappear as a function of temperature and then LFA signal should not exist at high temperatures. Disappearance of long range order is strongly associated with magnetization processes of the magnetic state. Microwave power was varied from P = 3 mW to P = 20 mW. The LFA signal strength was observed to be increasing significantly in response to microwave power increment provided that H_{DC} was parallel to film surface. Microwave power increment was done so as to verify correlation between LFA and magnetoimpedance (MI) experimentally since microwave power increments result in sudden microwave power loss in the film. These are basically the ohmic losses as a result of impedance (Z). Microwave power measurements were also done when the DC field was normal to the film surface so as to find contributions of anisotropy field. The DC field was modulated with a superposed AC field whose amplitude was varied between 10 Oe and 60 Oe at 100 KHz

frequency. The LFA signal strength was noted to be increasing significantly as the DC field was modulated only when H_{DC} is parallel to film surface showing contributions of anisotropy field.

The results to be discussed reveal that the LFA signal strength depends strongly on the DC field, temperature, microwave power and the orientation of the DC field with respect to the film surface. This anisotropy field says a lot about the ferromagnetic state of a material

This chapter presents and discusses the results of this study.

5.2: Bulk magnetization hysteresis measurement, ferromagnetic resonance (FMR) and low-field microwave absorption (LFA) measurements

Fig. 1 (a) shows bulk magnetization hysteresis measurement at T = 300 K, direct current DC as taken by SQUID magnetometer. Between 500-1000 Oe almost all of the magnetic moments are aligned in the direction of the field and an additional increase in the DC static magnetic field H_{DC} will yield very little increase in magnetization. This is called magnetic saturation. When H_{DC} is reduced to zero, it can be seen that the film remains magnetized. This is termed as a point of retentivity. At this point some of the magnetic moments remain aligned but some have lost their alignment. As the H_{DC} is reversed, the curve move to the point where magnetization M = 0. This is the point of coercivity, from the curve coercive force ($\approx$100 Oe) a behavior similar to most soft ferromagnets. As the H_{DC} is increased in the reverse direction the film will again become magnetically saturated but in the reverse direction. Again when H_{DC} is reduced to zero, it can be seen that the film remains magnetized. Our films are highly permeable as evidenced by the narrow width of the curve. Magnetoimpedence (MI) strongly depends on the penetration depth of the electromagnetic field on the permeability of the material.

Fig. 1 (b) Shows the derivative of microwave absorption dP/dH vs H_{DC} plot with measurements taken at temperature T = 293 K, microwave power P = 16 mW, and DC static magnetic field H_{DC} parallel to film surface. The dP/dH vs H_{DC} plot exhibited two absorptions

which can be associated with two different processes: one centered about $H_{DC} = 0$ that is more distinct and the other with a resonant field of ≈ 930 Oe. The former corresponds to the low-field microwave absorption (LFA) while the later denotes ferromagnetic resonance (FMR). Ferromagnetic resonance (FMR) is due to absorption in the full saturation state. This fact is supported by bulk magnetization hysteresis measurement at temperature T = 300 K shown in Fig. 1 (a). Low-field microwave absorption process (LFA) usually originates from the magnetization processes far from the saturation state also supported by bulk magnetization shown in Fig. 1 (a). The low-field microwave absorption signal (LFA) is opposite in phase with respect to that of ferromagnetic resonance (FMR). This indicates that the LFA has microwave absorption minimum at zero field in contrast to the microwave absorption maximum for the FMR line at its resonance field. This is analogous to LFA in Co-based ribbons as reported by Montiel et al [2] and Valenzuela et al [3]. LFA is understood to be connected to the magnetization processes that occur at low field region. We therefore assume that magnetization processes is present in the low field region centered at $H_{DC} = 0$. We attribute such magnetization processes to be due to the interaction of magnetic moments of thin films of FeSi with magnetic-field component of electromagnetic radiation. We could not observe hysteresis centered about $H_{DC} = 0$ on the dP/dH vs H_{DC} plot due to limitations of the Jeol ESR spectrometer which could not capture the reverse sweep data, though we actually see hysteresis along with the reverse sweep data on the instrument computer screen. However in Fig 1(a) we show the 300 K low-field hysteresis loop for the magnetization indicating that our film is definitely magnetic at room temperature.

At higher field $H_{DC} \approx 930$ Oe, we associate such field with ferromagnetic resonance (FMR), satisfying the Larmor relationship, as derived for the case of a thin sheet with negligible anisotropy field within the sheet plane (Eq. 3.7.5.1). Where ω_0 is the microwave angular frequency (with $\omega_0 = 2\pi f_0$ and $f_0 = 9.4$ GHz, γ is the gyromagnetic ratio, H_{dc} is the static magnetic field, and M is the magnetization. At the resonance condition, $M = M_s$ and $H_{dc} = H_{res}$. In this case the resonant field $H_{res} = 930$ Oe. By assuming a free electron behavior (Lande factor g = 2.0023), and $\gamma = 1.76 \times 10^7$ rad / s / G for spin-only behavior. The saturation

magnetization of the surface of the sample can be calculated from the resonance conditions as $M_S = 890$ G

Valenzuela et al [3] and Montiel et al [4] have done detailed studies on Co-based amorphous ribbons and alloys and both showed a good correlation between the low-field hysteresis in magnetization, magnetoimpedance (MI) and low-field microwave absorption (LFA). Both Valenzuela et al [3] and Montiel et al [4] showed experimentally that the maxima in the MI curve coincide with the minimum and maximum of the LFA curve. This therefore concludes common origin of both processes, essentially controlled by anisotropy field. The shape and peak to peak width of LFA signal also depends on the microwave frequency as said by Lee et al [5] in Co thin films. Lee et al [5] attribute LFA to the presence of magnetic domains in the unsaturated state of the material. Carara et al [6, 7] show that MI strongly depends on the evolution on the domain structure in $FeSi_{3\%}$. A very high MI up to 360% at 100 KHz has been obtained in $FeSi_{3\%}$ samples. The fact that LFA is well correlated with MI in this study is a positive signature of magnetic state in the FeSi thin films.

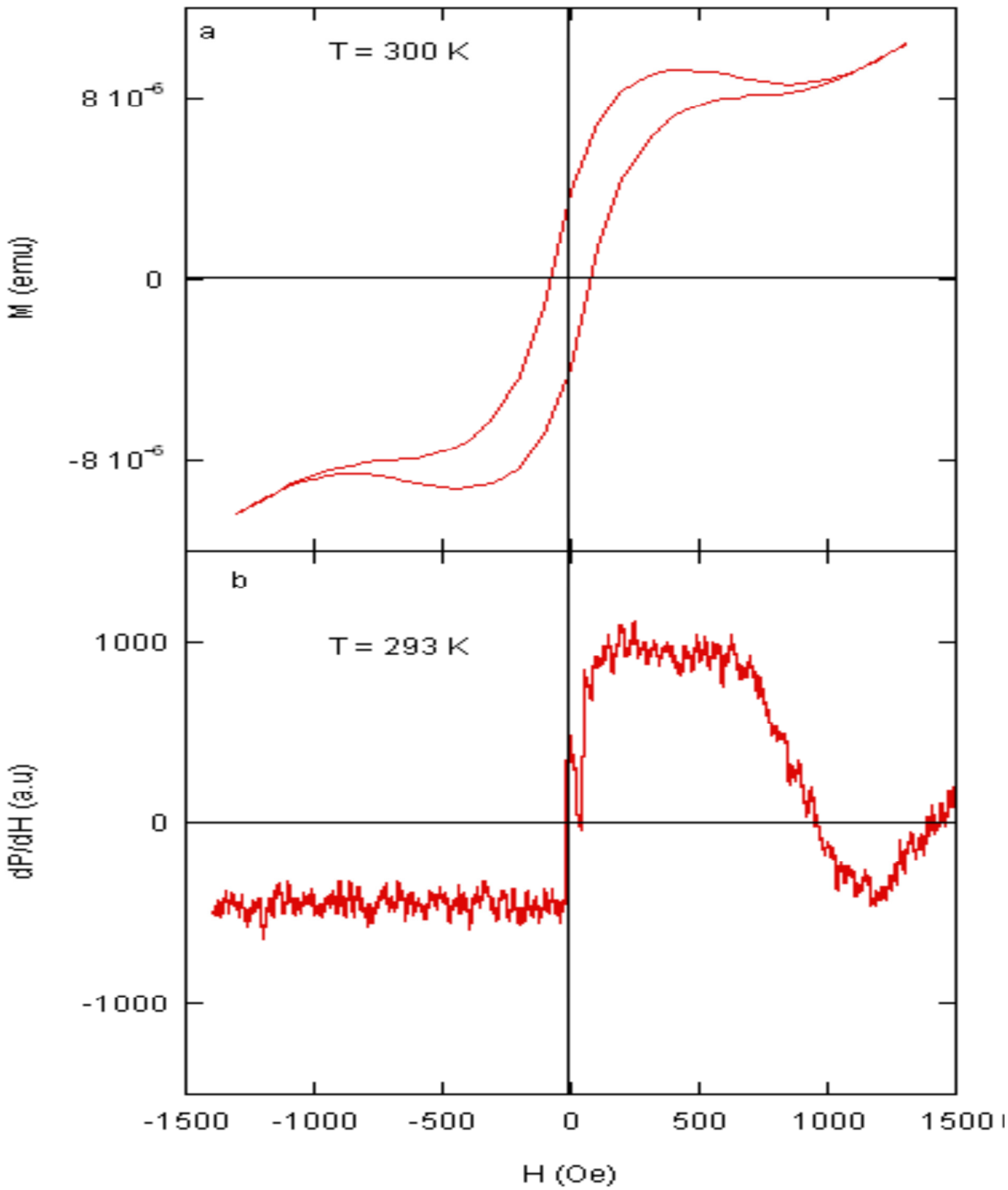

Fig. 1. (a) Bulk hysteresis measurement taken at T = 300 K, (b) The low-field microwave absorption measurements taken at temperature T = 293 K with microwave power P = 16 mW and DC field parallel to the FeSi film surface.

5.3: Angular dependence of low-field microwave absorption analysis.

Angular dependence of low-field microwave absorption (LFA) on the mutual orientation of the DC static magnetic field H_{DC} and the film surface help us to study the role of anisotropy field on the LFA signal. Fig. 2 shows the variation of the derivative of microwave absorption with angle from $\vartheta = 0°$ to $\vartheta = 90°$ for thin film of FeSi. Measurements were carried out at temperature T = 293 K and microwave power P = 16 mW while the microwave magnetic field H_{MW} was kept parallel to the surface of the film. The DC static magnetic field H_{DC} with respect to film surface was varied from $\vartheta = 0°$ (H_{DC} parallel to film surface) to $\vartheta = 90°$ (H_{DC} normal to film surface). At $\vartheta = 0°$ the intensity of the LFA signal is quite significant and may be due to the induced anisotropy field (IAF) since magnetization remains within the plane. Induced anisotropy field (IAF) corresponds to the energy needed to orientate the magnetic moments in the easiest direction. When the DC static magnetic field is parallel to the film surface it coincides with easy magnetization axis. A slight difference in the intensity of the LFA signal is observed between $\vartheta = 0°$ to $\vartheta = 30°$ since induced anisotropy field (IAF) is still dominant. This therefore implies that magnetic moments are still aligned in the easy axis. The intensity of the signal decreases significantly in the angular variation of $60° \le \vartheta \le 90°$ due to effects of shape anisotropy field (SAF).

Shape anisotropy field (SAF) corresponds to the energy needed to orientate magnetic moments in the hardest direction. SAF is maximum at $\vartheta = 90°$ since magnetization is out of the plane, however at $\theta = 0°$ it is minimum since magnetization remains within the plane [8]. It can be said that for angular variation of $0° \le \vartheta \le 90°$ both the shape anisotropy field (SAF) and induced anisotropy field (IAF) contributes to total anisotropy field (TAF). It can be observed that TAF plays a significant role in low-field microwave absorption (LFA) in our films and is in good agreement with the scenario given by Alvarez et al [9] and Montiel et al [2, 8]. It should be noted that crystals of ferromagnetic materials and ferrites have easy and difficult directions of magnetizations and hence such strong dependence of low-field microwave absorption (LFA) signal on the orientation of DC static magnetic field H_{DC} with respect to the film surface is a signature of a ferromagnetic state of a material.

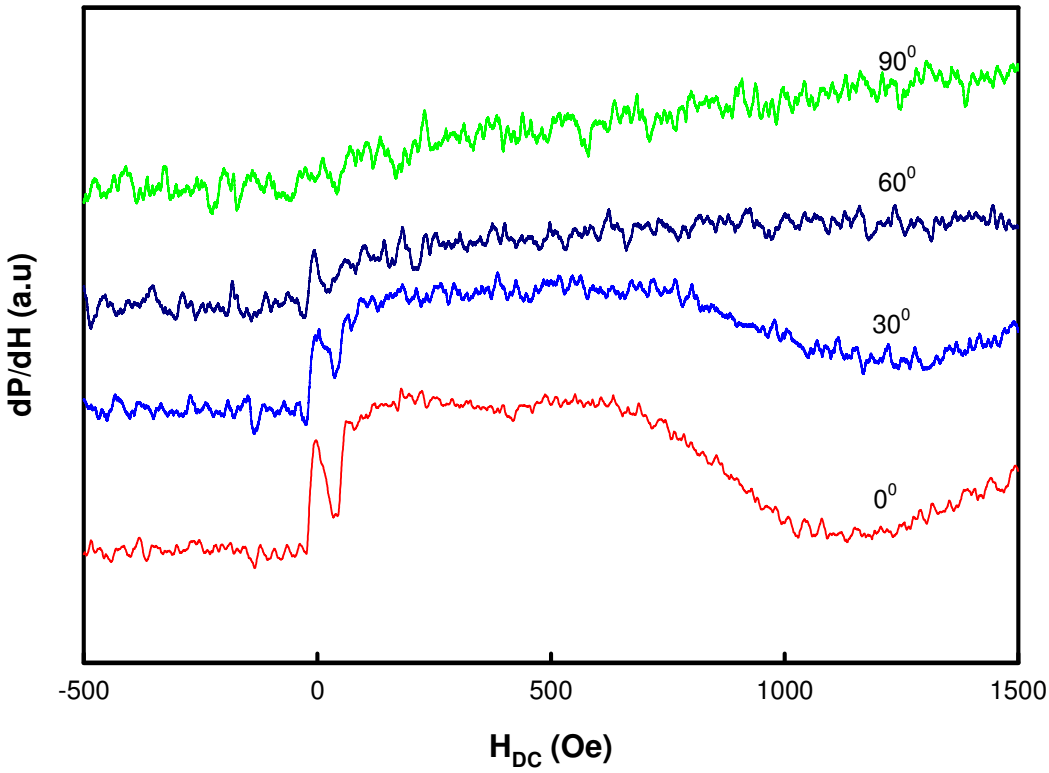

Fig. 2 The angular dependence of low-field microwave absorption measurements of FeSi film taken at T = 293 K with microwave power P = 16mW.

5.4: Temperature dependence of low-field microwave absorption analysis

Anisotropy and other magnetic parameters are a function of temperature. In most ferromagnetic materials induced magnetization decreases when temperature increases [10]. At higher temperatures disorder is mainly produced by the interaction of electrons with ions. In ESR the intensity of the signal is lowered by increasing the temperature. The distribution of electron between the two states is given by the Maxwell- Boltzmann expression (Eq. 3.31)

As the temperature increases more spins will be in the upper state, difference between n_1 (electrons in the upper state) and n_2 (electrons in the lower state) is lowered and hence net absorption decreases. Decrease in net absorption implies decrease in magnetization in the region

H_{DC} = 0. We assume that low-field microwave absorption centered at H_{DC} = 0, ΔE = 0, however due to the effects of hysteresis at H_{DC} = 0, splitting of energy levels is inevitable therefore (Eq. 3.3.1) holds. We could not observe hysteresis on our LFA spectra due to the limitations of our machine which could not capture the reverse sweep data, though we actually see hysteresis along with the reverse sweep data on the instrument computer screen.

If this LFA observed in thin films of FeSi is a signature of ferromagnetic state then the long range order should disappear as a function of temperature and then LFA signal should vanish at high temperatures as illustrated by (Eq. 3.3.1). Fig. 3 shows the variation of the derivative of the microwave absorption with temperature for the thin film FeSi. Measurements were carried out from temperature T = 293 K to T = 370 K and microwave power P = 16 mW. DC static magnetic field was parallel to the film surface.

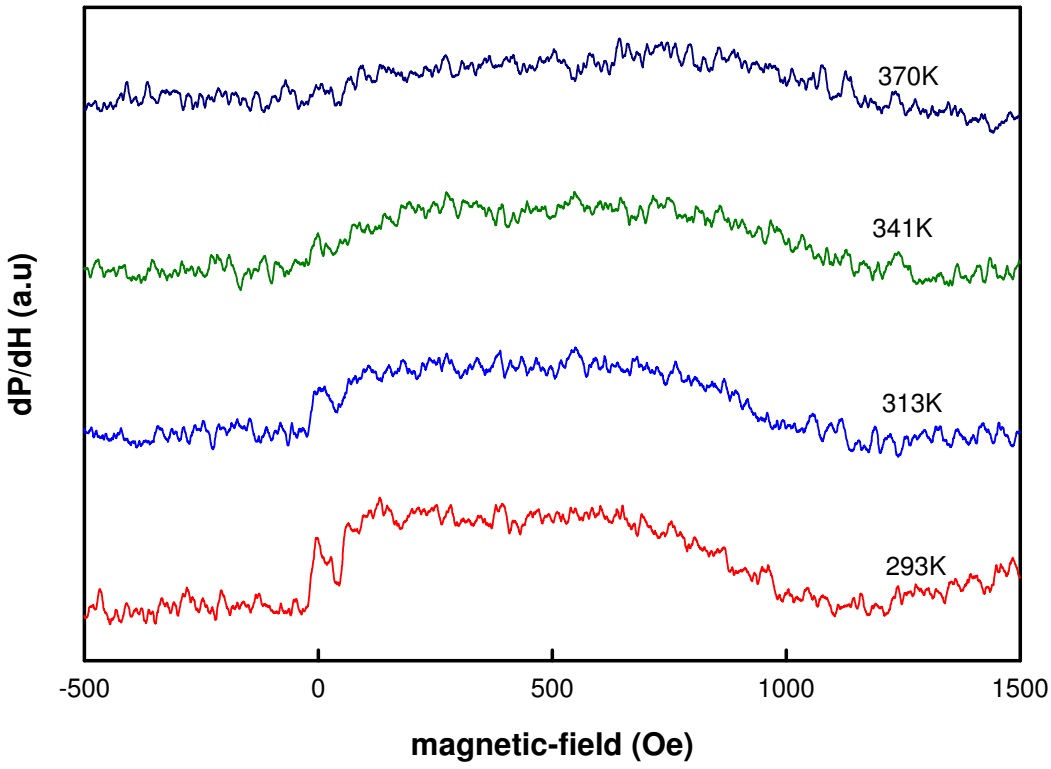

Fig. 3: Temperature dependence of low-field microwave absorption from T = 293 K to T = 370 K. and microwave power P = 16 mW with DC field was parallel to the film surface for FeSi film.

The LFA spectra is only significant at temperatures T =293 K and T = 313 K. Beyond T = 313 K, absorption centered at zero field is almost negligible and completely disappears at 340 K. We can conclude the possibility of 340 K being the Curie temperature (T_C) of this film. The disappearance of the absorption signal at T = 340 K is clearly illustrated in Fig. 4 below.

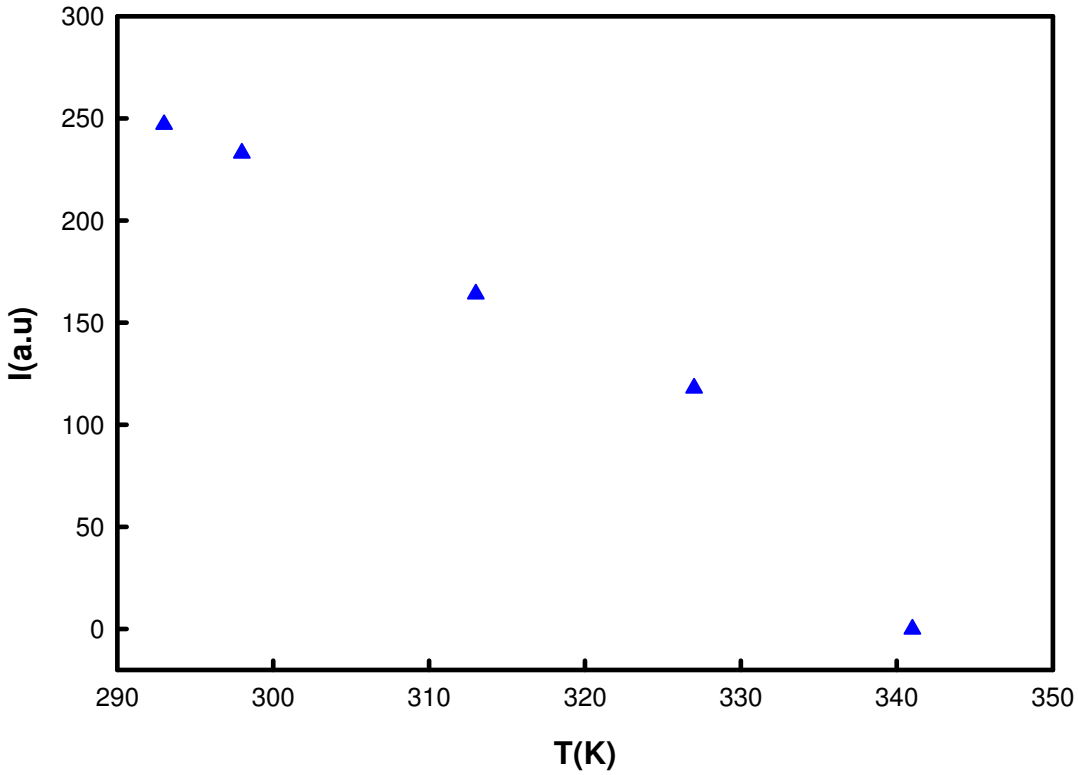

Fig. 4: Temperature dependence of the intensity I of the dP / dH signal near $H_{DC} = 0$

The disappearance of LFA signal in our film at 340 K correlates with the arguments of Alvarez et al [11] that it is indicative of disappearance of long range order and is strongly associated with magnetization processes of the magnetic state. The long range order which create magnetic domains in ferromagnetic materials is due to quantum mechanical interaction at the atomic level. This interaction result in locking of magnetic moments of neighboring atoms into a rigid parallel order over a large number of atoms in spite of temperature increment which tends to randomize any atomic level order. Beyond 340 K the long range order abruptly disappears. However we should also take into consideration the origin of LFA from the formation of ferromagnetic clusters in these films. Such ferromagnetic clusters can disappear at high temperatures and thus

lead to the disappearance of LFA. Either way, LFA disappearance as a function of temperature indicates its association with some sort of long range order.

5.5: Microwave power dependence of low-field microwave absorption

The number of unpaired electrons in thin film of FeSi is proportional to the amount of energy absorbed in electron spin resonance (ESR). The amplitude of the spectra quantifies the amount of microwave absorption by the cavity. This therefore implies that the number of the spins is the integral value of the spectral intensity. The spectral intensity I is directly proportional to the square root of the microwave power P absorbed i.e. $I\alpha\sqrt{P}$. Increasing the microwave power increases the net absorption of microwave radiation by the spins. It should also be noted that increasing the microwave power increases the microwave power loss in the film. These are basically ohmic losses, which are due to impedance. Effects of surface anisotropy field (SAF) and induced anisotropy field (IAF) also play a central role in the determination of spectral intensity.

Fig. 5 shows the variation of the derivative of the microwave absorption with microwave power for the thin film FeSi. Measurements were carried out from microwave power P = 3 mW to P = 20 mW at temperature T = 293K. The DC static magnetic field H_{DC} was parallel to the film surface. LFA signal showed a significant increase in the intensity of microwave power from 3mW to 20 mW. This shows that microwave power variation has major contribution to the change in the intensity of the absorption spectra. Experimentally as we increase the microwave power, the microwave magnetic field H_{AC} intensity in the sample cavity increases. The increased H_{AC} induces more microwave currents on the film surface leading to increased microwave power loss in the film. These are basically the ohmic losses, which are due to impedance (Z). This again is in good agreement with the scenario that low-field microwave absorption (LFA) and magnetoimpedance (MI) has common origin as described by Montiel et al [4]. Moreover this shows the validity of (Eq. 3.7.2.10) that shows a theoretical correlation between LFA and MI.

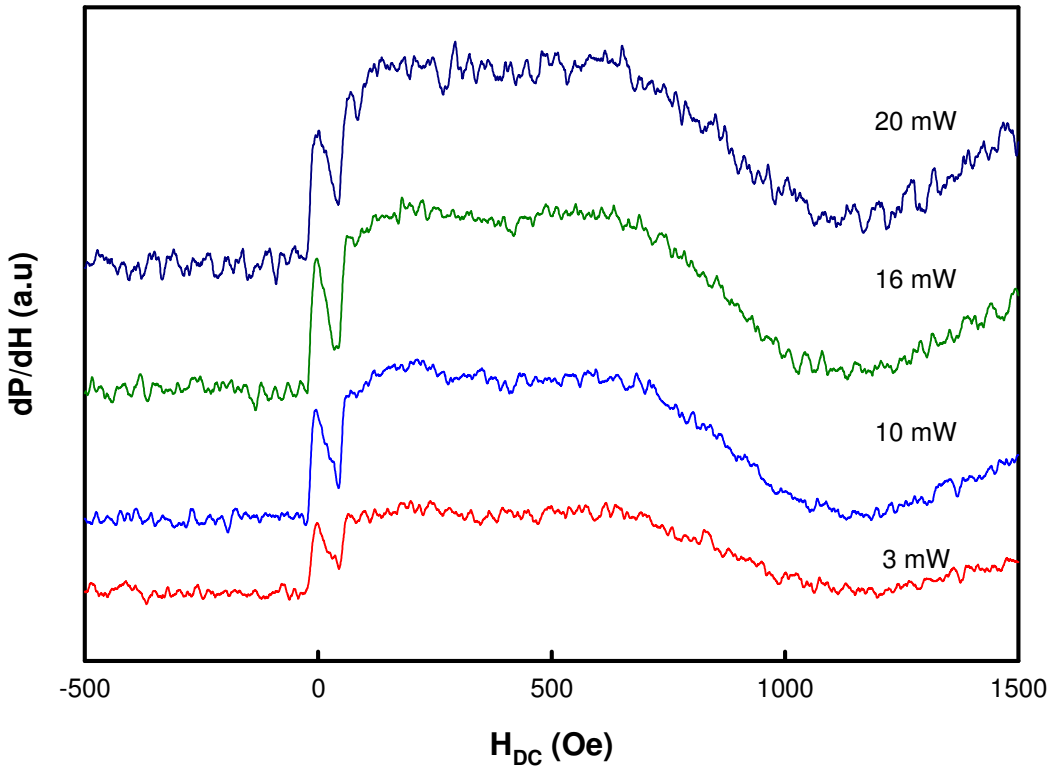

Fig. 5: The microwave power dependence of low-field microwave absorption measurements taken at T = 293 K with DC field was parallel to the film surface for FeSi film.

To study the role of anisotropy further, the DC static magnetic field H_{DC} was aligned normal to film surface as shown in Fig. 5. Measurements were carried out from microwave power P = 3 mW to P = 20 mW at temperature T = 293K. The intensity of the LFA spectra decreased significantly from 3 mW to 20 mW. This is a clear indication that the direction of orientation of the film to the DC static magnetic field contributes to a greater extent to the nature of absorption spectra formed. Microwave power increment plays a central role when the DC field is aligned parallel to the film surface in LFA. Shape anisotropy field (SAF) was at maximum due to normal orientation of the film surface to DC static field. Induced anisotropy field (IAF) was almost negligible. SAF mainly contributed to total anisotropy field (TAF).

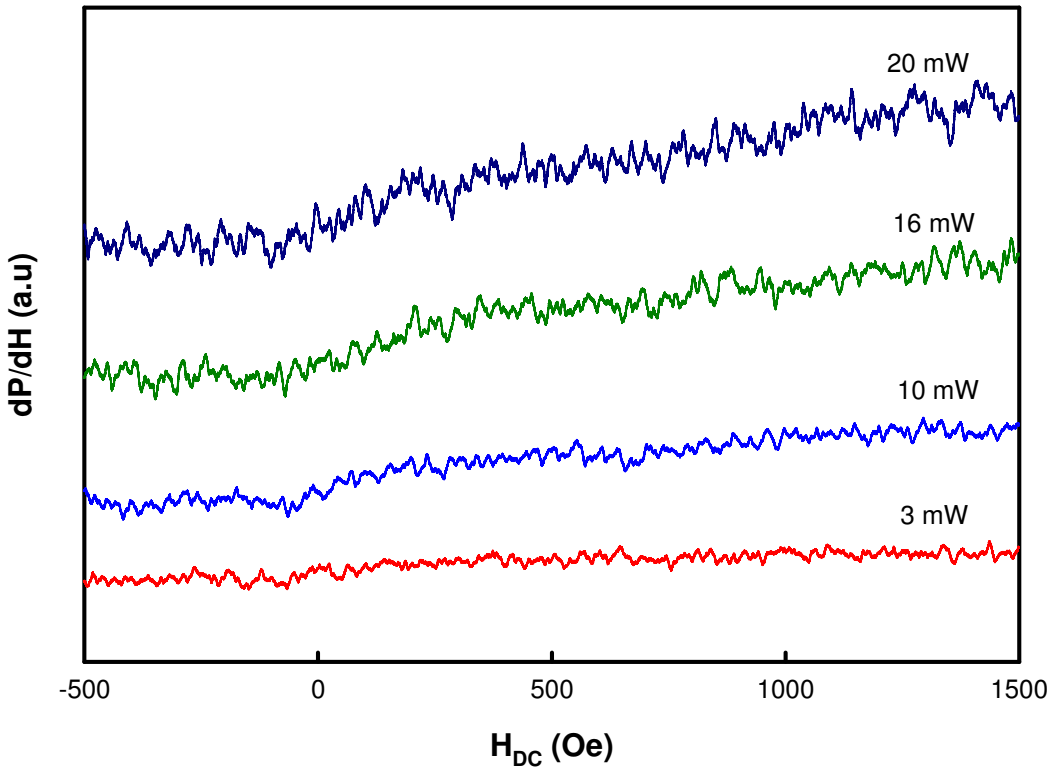

Fig. 5: The microwave power dependence of low-field microwave absorption measurements taken at T = 293 K with DC field was normal to the film surface for FeSi film.

5.6: DC modulation field dependence of low-field microwave absorption

DC modulation depends on the superimposition of a small amplitude sinusoidal magnetic field B_1 to the DC static magnetic field H_{DC}. This technique allows amplification of the ESR signal [12]. DC field modulation increases the sensitivity of the ESR method and hence lowers minimum number of detectable spins. Minimum number of the detectable spins from the thin film is given by (Eq. 4.8.1).

However despite DC field modulation, effects of the anisotropy field have a central influence on the LFA shape since when DC static magnetic field is aligned normal to the film surface LFA signal diminishes. Fig. 6 shows the variation of the derivative of the microwave absorption with

DC modulation field. Measurements were carried out from 10 Oe, 30 Oe and 60 Oe, 16 mW and at 293 K. DC static magnetic field was parallel to film surface. Significant variation in the intensity of the spectra is shown from 10 Oe to 60 Oe indicating strong dependence of LFA spectra on the DC magnetic field modulation, a clear indication that the number of detectable spins increases significantly as the DC modulation field is increased. At 10 Oe the intensity and the width of the spectra is almost negligible. A dominant absorption signal is shown at 60 Oe revealing greater net absorption by the spins. For parallel orientation SAF is a minimum since magnetization is within the plane, and the magnetization effect is enhanced by modulating the DC field. Induced anisotropy field IAF contributes to total anisotropy field TAF in this case since FeSi film is completely parallel to the DC static field.

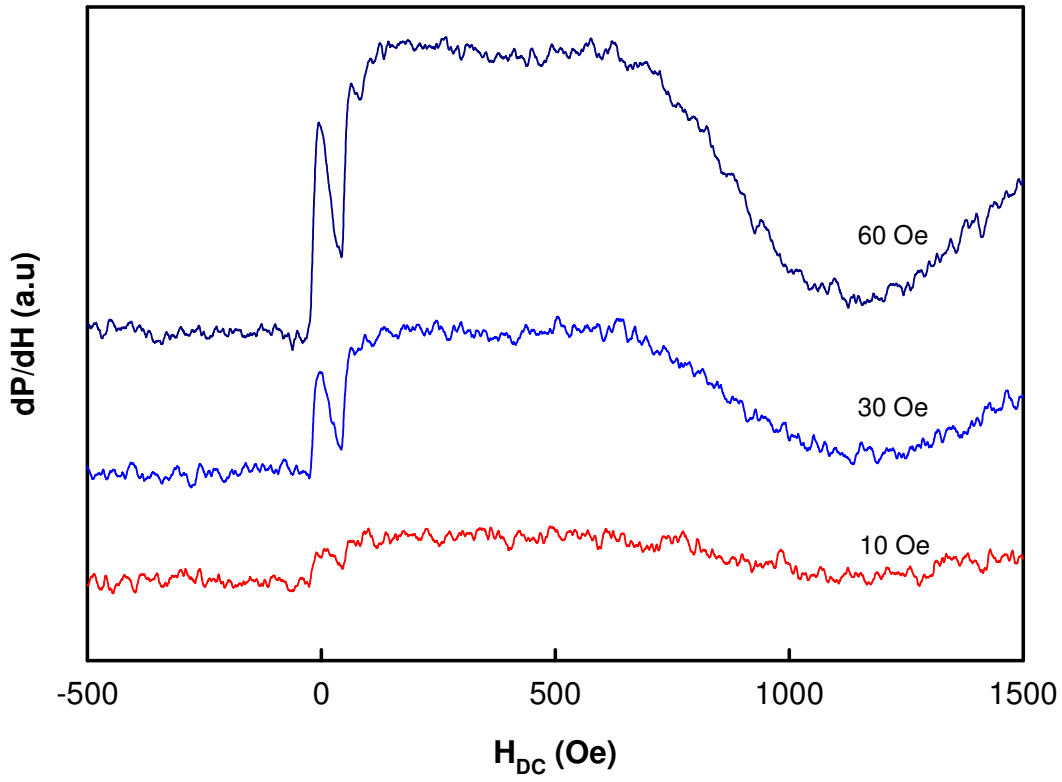

Fig. 6: The DC modulation field dependence of low-field microwave absorption measurements taken at T = 293K with microwave power P = 16 mW and DC field was parallel to the film surface of the film.

To study the role of anisotropy further, we aligned our film surface normal to the DC static magnetic field. Despite modulating the DC static field the LFA signal was almost insignificant in this alignment showing strong influence of the anisotropy field to the LFA signal strength. In this alignment surface anisotropy field (SAF) contributes predominantly to the LFA shape. SAF contributes to TAF. This therefore explains the significant decrease in the intensity of the LFA signal as compared to parallel orientation. This behavior of the variation of the derivative of the microwave absorption with DC modulation field for the film is shown in Fig. 7 shows, where the measurements were carried out from 10 Oe to 60 Oe, 16 mW and at 293 K with DC static magnetic field was normal to the film surface.

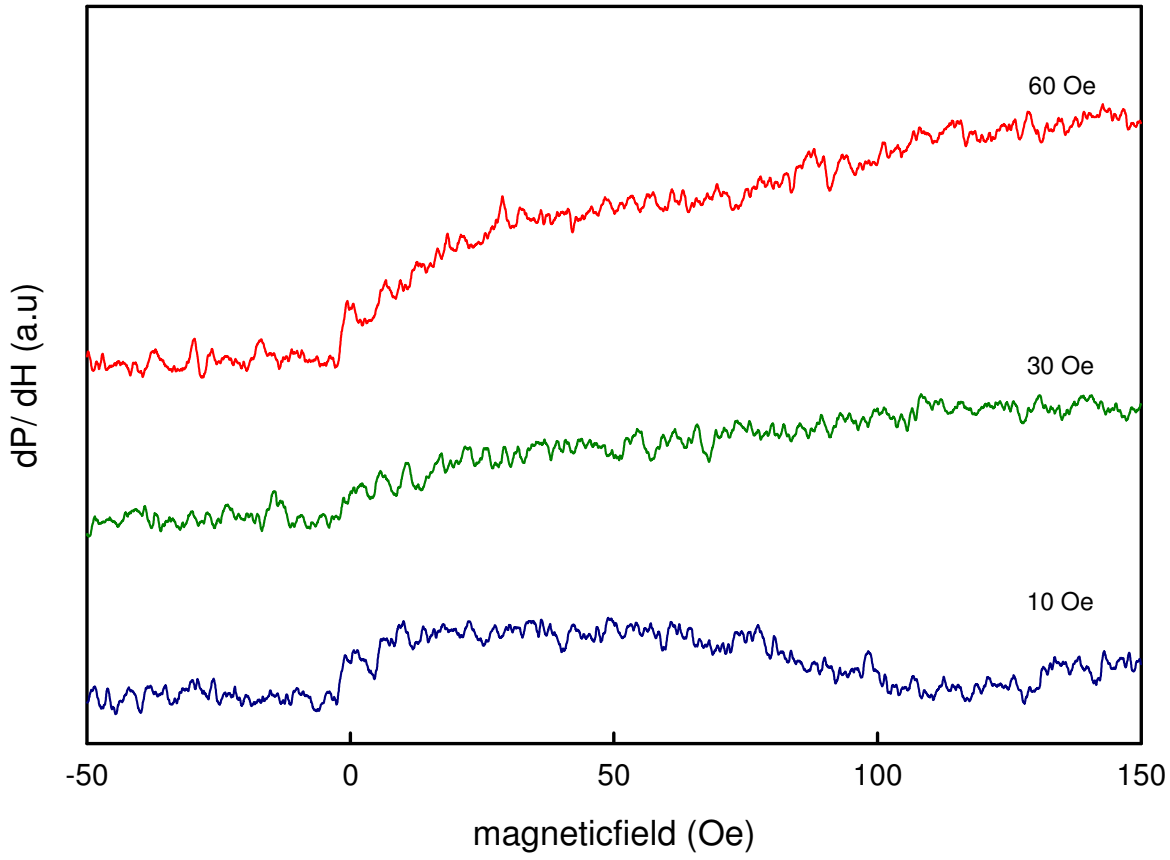

Fig. 6: The DC modulation field dependence of low-field microwave absorption measurements taken at T = 293K with microwave power P = 16 mW and DC field was normal to the film surface of the film.

5.7: Conclusions

We have observed LFA signal for the first time in good quality polycrystalline B20 cubic structure FeSi thin films grown by PLD on Si (111) substrate. The main feature observed in all spectra is that the anisotropy field has a central influence on the LFA signal strength. Magnetic anisotropy is a signature of ferromagnetic state of a material. The observed LFA signal strongly depends on the mutual orientation of H_{DC} and the film surface and disappears at high angles. We qualitatively analyzed these features in terms of total anisotropy. Thus, the observation of LFA and its strong dependence on the orientation of DC field with respect to film surface gives a positive evidence of magnetic state even at room temperature and above in these films. Further the LFA signal disappears at high temperatures and can be attributed to the disappearance of long range order giving additional proof of a magnetic state in these films at room temperature and beyond. The LFA signal strength increases with the increase of microwave power, giving additional evidence that the LFA has common origin with MI as reported in the literature. MI and LFA can be understood as the absorption of electromagnetic radiation by spin systems that are modified by domain evolution and strongly depend on the anisotropy field. We believe that domain structure evolution in low fields, which in turn modifies the low field permeability as well as the anisotropy, could be the origin of the LFA observed in these films. We also believe that the hysteresis observed can be due to different irreversible domain configurations occurring caused by cycling the DC field. The observation of LFA signal of FeSi thin films makes them potential candidates for application as low magnetic field sensors in the microwave and rf frequency regions. Ferromagnetic thin films of FeSi are promising as magnetic-silicide system for polarized current production, manipulation and detection.

References

[1] N.Manyala, B.Ngom, A.Beye, R.Bucher, M.Maaza, A. Strydom, A. Forbes, A. Johnson and J. DiTusa, Appl.Phys.Lett.**94**, 232503 (2009).

[2] H. Montiel, G. Alvarez, I. Betancourt, R. Zamorano, R. Valenzuela, and R. Zamorano, Superficies y Vacio **19,** 3 (2006).

[3] R.Valenzuela, H.Montiel, G.Alvarez, and R.Zamorano, Phys.Status Solidi. **206,** 652-655 (2009).

[4] H. Montiel, G. Alvarez, I. Betancourt, R. Zamorano, R.Valenzuela, Appl. Phys. Lett. **86**, 072503 (2005).

[5] S. Lee, C. Tsai, H. Cho, M. Seo, T. Eom, W. Nam, Y. Lee and J. Ketterson, J. Appl. Phys. 106, 063992 (2009).

[6]. M. Carara, A. Gundel, M. Baibich and R. Sommer, J. Appl. Phys. 84, 3792 (1998).

[7]. M. Carara and R. Sommer, J. Appl. Phys. **81**, 8 (1997).

[8] H. Montiel, G. Alvarez, R. Zamorano, and R. Valenzuela, J. Non-Cryst.Solids **353,** 908-910 (2007).

[9] G. Alvarez, H. Montiel, D. de Cos, A. Garcia-Arribas, R. Zamorano, J. Barandiaran, and R. Valenzuela, J. Non-Cryst.Solids **354,** 5195-5197 (2008).

[10] F.Brailsford, Physical Principles of Magnetism, Butler and Tanner Ltd, London, (1966).

[11] G. Alvarez, H. Montiel, J.F. Barron, M.P. Gutierrez and R. Zamorano, J.Magn.Magn. mater, 322, 348 (2010).

[12] J.Weil and J. Bolton, Electron Paramagnetic Resonance, second edition. J. Wiley, USA, (2007).